Three wave interactions in non-degenerate and degenerate magneto-plasmas

A thesis submitted in partial fulfillment of the requirement for the award of degree of
Doctor of Philosophy in Physics

By

Muhammad Shahid
Reg. No. 088-GCU-PHD-PHY-08

Department of Physics
GC University Lahore

رَّبِّ زِدْنِي عِلْمًا

My Lord! Increase me in knowledge.

[Quran 20:114]

TO

The sweet memories of my First School

(Government Primary School, Pind Suleman Makhan, Tehsil & District Attock)

Research Completion Certificate

It is certified that the research work contained in this thesis entitled "**Three wave interactions in non-degenerate and degenerate magneto-plasmas**" has been carried out by ***Mr. Muhammad Shahid*** Reg. No. 088-GCU-PHD-PHY-08 under my supervision at Physics Department, GC University Lahore, during his postgraduate studies for ***Doctor of Philosophy in Physics.***

Supervisor

Prof. Dr. G. Murtaza(S.I.)
Salam Chair in Physics
GC University, Lahore

Submitted Through

Prof. Dr. H. A. Shah(S.I.)
Chairperson
Department of Physics
GC University, Lahore

Declaration

I, **Mr. Muhammad Shahid**, Reg. No. 088-GCU-PHD-PHY-08, PhD scholar at the Department of Physics, GC University Lahore, hereby declare that the matter printed in the thesis entitled "**Three wave interactions in non-degenerate and degenerate magneto-plasmas**" is my own work and has not been printed, or published or submitted as research work, thesis or publication in any form in any University/Research Institution etc. in Pakistan or abroad.

Dated: 20 Feb 2014 _____

Signature of Deponent

Acknowledgements

All praise to ***Almighty Allah,*** *the most* gracious *and merciful, who enabled me to complete this research work successfully.*
First of all, I would like to express my sincere gratitude to my supervisor **Prof. Dr. G. Murtaza** for his guidance and continuous support. His thought provoking discussions broadened my views and understanding of the subject. He was always there to listen and to give his point of view. He not only introduced me to the subject of plasma physics but also nurtured me as a researcher.

I am also indebted and very grateful to my collaborator ***Prof. D. B. Melrose*** for his invaluable guidance during my stay at University of Sydney, Austraila. He particularly taught me how to design and tackle a research problem.

Prof. Dr. H. A. Shah, Chairman Department of Physics deserves special thanks for providing sound working environment and good facilities at the Department of Physics, GC University, Lahore.

I would especially like to thank all my friends and co-workers for stimulating and helpful Discussions.
I express my deep gratitude to Salam Chair in Physics, GC University Lahore, Pakistan. Higher Education Commission of Pakistan and the Abdus Salam International Centre for Theoretical Physics, Trieste, Italy, for financing some part of my doctoral research.
With memories, I would like to thank ***Prof. Saeed Ahmad*** (Govt. College Attock) for his visionary guidance throughout my study, and ***Prof. Abdul Jabbar*** (Govt. College Attock) for his inspiring physics teaching at Intermediate level which accelerated me to study the physics at higher level. My friends Ismail Mubashir and Ejaz Ahmad Chughtai always encouraged me to go abroad for study. Therefore, I spent six months in University of Sydney Australia for partial PhD research and enjoyed a memorable tour.
Last but not the least; I am enormously grateful to my loving parents, my brothers and other family members who always pray for my success in every aspect of life. I would especially like to thank one of my brothers, Muhammad Zahid who cared a lot for me during my academic career. I am profoundly thankful to my caring wife for her patience and understanding during the progress of this work. Many many loves for my cute baby son Usman.

Muhammad Shahid

List of Publications

Publications included in this thesis

1. Spin effect on parametric interactions of waves in magnetoplasmas,
   M. Shahid, D. B. Melrose, M. Jamil, and G. Murtaza, Phys. Plasmas **19**, 112114 (2012).
2. Spin effect on parametric decay of oblique Langmuir wave in degenerate magneto-plasmas,
   M. Shahid and G. Murtaza, Phys. Plasmas, **20** 082124 (2013).
3. A comparison of parametric decay of oblique Langmuir wave in high and low density magneto-plasmas,
   M. Shahid, A. Hussain, and G. Murtaza, Phys. Plasmas, **20** 092121 (2013).

Publications not included in this thesis

1. The parametric decay of dust ion acoustic waves in non-uniform quantum dusty magnetoplasmas,
   M. Jamil, **M. Shahid**, Waris Ali, M. Salimullah, H. A. Shah, and G. Murtaza, Phys. Plasmas **18**, 063705 (2011).

2. Quantum modification of dust shear Alfven wave in plasmas,
   M. Jamil, **M. Shahid**, I. Zeba, M. Salimullah, H. A. Shah, and G. Murtaza, Phys. Plasmas **17**, 054504 (2010). Phys. Plasmas **19**, 023705 (2012).

3. **M. Shahid,** Z. Iqbal, A. Hussain, and G. Murtaza, *R- and L-Waves in Electron-Positron Spin Quantum Plasmas,* partially accepted in **Physica Scripta**.

Abstract

In this thesis we study the parametric decay instability problem (three wave interactions) in classical and quantum magneto-plasmas. Two combinations of the three wave interactions have been investigated. First, the parametric decay instability of upper hybrid wave into low-frequency electromagnetic shear Alfven wave and Ordinary mode radiation has been solved in an electron-ion plasma immersed in uniform external magnetic field. Incorporating quantum effect due to electron spin, the fluid model has been used to investigate the linear and nonlinear response of the plasma species. It is shown that the spin of electrons has considerable effect on the three-wave coupling interactions even in classical regime.

Secondly, the electron spin -1/2 effects on the parametric decay instability of oblique Langmuir wave into low-frequency electromagnetic shear Alfven wave and left-handed circularly polarized wave (LHCP) has been investigated in an electron-ion quantum plasma immersed in uniform external magnetic field. Incorporating the quantum effects due to electron spin, Fermi pressure and Bohm potential term, the quantum magneto-hydrodynamic (QMHD) model has been used to investigate the linear and nonlinear response of the plasma species for three-wave coupling interaction in a quantum magneto-plasmas. Nonlinear dispersion relations and growth rates have been derived analytically. It has been shown that the spin of electrons has considerable effect on the growth rate of parametric instability problem even when the external magnetic field B_o is below the quantum critical magnetic field strength $B_Q = 4.4138 \times 10^{13} G.$

Finally, the parametric decay instability of oblique Langmuir wave into low-frequency electromagnetic shear Alfven wave and LHCP have also been investigated in high density (quantum) and low density (classical) magneto-plasma environments. QMHD model has been used to find the linear and non-linear response of the high density quantum magneto-plasma, and to compare the results with the low density classical plasma we have used classical limit $(\hbar \to 0,\ P_e \to P_{te})$ in the results of QMHD model. Nonlinear dispersion relations and growth rates of the problem have been derived analytically. The growth rate both for quantum and classical magneto-plasma environments has been plotted. The normalized growth rate as a function of number density in the high density degenerate magneto-plasmas increases exponentially while in the low density classical magneto-plasmas it increases logarithmically.

Contents

List of Figures

Chapter 1

Introduction

It is believed that we live in 1% of the universe where plasma does not exist naturally and 99% of the matter in the visible universe is in the plasma state [1]. About 84 years ago Tonks and Langmuir (1929) first coined the term 'plasma' to describe the inner region of a glowing ionized gas produced by means of an electric discharge in a tube [2]. Plasma may be defined as a gas of charged and neutral particles which behave collectively via electromagnetic fields. To understand the collective behavior of plasma, let us decompose the electric field due to charge separation in plasma into two parts (E_1 and E_2) which have distinct spatial scales. The E_1 field has spatial variations on a scale length much less than the electron Debye length, which is the length over which the field of an individual charge is shielded out by the response of the surrounding charge particles. Due to random collisions among the discrete charges, E_1 becomes rapidly fluctuating micro-field. On the other hand, E_2 represents the field due to separation of charges over space scales greater than or comparable to the Debye length. This field is responsible of 'collective' or coherent motion of the charges. Thus plasma has a natural separation into collisional and collective behavior. The collisional behavior becomes negligible when the number of electrons in Debye sphere becomes very large [3].

Plasma does not always exist in electron-ion form. Indeed, in most cases plasma coexists with the charged dust particulates. An admixture of such charged dust, electrons, ions, and neutrals form a 'dusty plasma'. In the last two decades, the electron-positron plasma, electron-positron-ion plasma, quark-gluon plasma have also been studied extensively. For high density regime of plasma where the average interparticle distance is equal or less than the thermal de

Broglie wavelength of the charged particles quantum effects become dominant. This plasma is called degenerate or quantum plasma. The plasma environments where the particle speed is greater than $0.86c$, relativistic corrections to particle's mass and velocity become important and plasma is called relativistic plasma. In this thesis we concern with classical electron-ion plasma and quantum electron-ion plasma.

1.1 Plasma Occurrence and Applications

Plasma exists naturally in many space and astrophysical environments like aurora, ionospheres and magnetospheres of planets, solar and stellar winds, solar atmosphere, shocks, flux ropes, coronal mass ejections, pulsars's magnetosphere, stars, interstellar medium, intergalactic medium, astrophysical jets, lightning, Ball lightning etc. Examples of the occurrence of plasmas on the earth are Fluorescent Lights, Spark gaps, arcs, welding, lighting, Controlled Fusion, Plasma discharge pumped lasers, plasma lenses for particle accelerators etc.

There is a wide range of plasma applications in different areas and some of them are outlined briefly below.

The thermal and chemical energy of plasmas is used in arc plasma processing, material fabrication, plasma chemistry, semiconductor processing and surface modification.

The kinetic energy of plasmas is used in magneto-hydrodynamic (MHD) power generation and propulsion in space to control the position and orientation of spacecraft.

The electromagnetic waves radiated from plasmas are used in light sources, laser pumping and in plasma display panels.

Another example is controlled thermonuclear fusion. Most of the energy sources on the Earth linked directly or indirectly to the sun. The energy in all stars including sun comes from the fusion of light elements. In 1940, researchers aimed at 'producing the energy of a star on Earth'. Unfortunately the first realization of this research came in the form of hydrogen bomb. Since that time, the research on the generation of controlled thermonuclear fusion for peaceful purposes has been carried out. With great effort of researchers in the development of plasma theory and technology, this ultimate energy source for the human race is expected to be realized within a generation.

1.2 Theoretical Analysis of Plasmas

Plasma is a gas of charged particles which behave collectively via electromagnetic fields. To describe the plasma theoretically, mainly there are two approaches one is kinetic approach and other is fluid approach. Kinetic approach is difficult but gives more insight while the fluid approach is simple one to handle. For simplicity in this thesis we restrict ourselves to use the fluid approach.

1.2.1 Fluid Model

The first assumption in the non-relativistic fluid model is the conservation of particles which states that free particles cannot be destroyed and cannot be created. The continuity equation is the result of this assumption which can be derived from the zeroth velocity moment of the Vlasov equation or the collisionless Boltzmann equation that is

$$\frac{\partial n_j}{\partial t} + \nabla.\left(n_j \mathbf{v}_j\right) = 0. \tag{1.1}$$

Next, the fluid volume in plasma will experience pressure and electromagnetic forces. We can obtain the non-relativistic momentum equation by multiplying the Vlasov equation with $m\mathbf{v}$ and integrating over velocity space as

$$m_j n_j \left(\frac{\partial}{\partial t} + \mathbf{v}_j.\nabla\right)\mathbf{v}_j = q_j n_j \left(\mathbf{E} + \frac{\mathbf{v}_j \times \mathbf{B}}{c}\right) - \nabla.\mathbf{P}_j \tag{1.2}$$

where $\mathbf{P}_j = \int m\mathbf{v}\mathbf{v} f_j d^3v$ is the pressure tensor and $\mathbf{E} + (\mathbf{v}_j \times \mathbf{B})/c$ is the electromagnetic force. Collisions between the plasma species have been neglected. In most of the plasma environments like Earth's magnetosphere, pulsar magnetosphere, solar and astrophysical plasmas etc., the electron-ion collision frequency is much smaller than the electron plasma frequency. So the collisionless fluid equations are valid for most of the plasma environments. For simplification, we replace the divergence of the pressure tensor with the gradient of a scalar pressure $P_j = n_j k_B T_j$. To describe the electrostatic and electromagnetic wave phenomenon in plasmas, the following

Poisson-Maxwell equations are used together with the continuity and momentum equations.

$$\boldsymbol{\nabla} \times \mathbf{E} = -\frac{1}{c}\frac{\partial \mathbf{B}}{\partial t} \tag{1.3}$$

$$\boldsymbol{\nabla} \times \mathbf{B} = \frac{4\pi}{c}\mathbf{J} + \frac{1}{c}\frac{\partial \mathbf{E}}{\partial t} \tag{1.4}$$

$$\boldsymbol{\nabla}.\mathbf{E} = 4\pi \sum_j q_j n_j \tag{1.5}$$

$$\boldsymbol{\nabla}.\mathbf{B} = \mathbf{0} \tag{1.6}$$

In this thesis, we have also used the non-relativistic quantum hydrodynamic equations in which the electron momentum equation includes the Bohm potential term and the quantum statistical pressure. The electron Fermi statistical pressure is

$$P_{Fe} = n_e k_B T_{Fe} \tag{1.7}$$

where $T_{Fe} = \hbar^2(3\pi^2 n_{0e})^{2/3}/2k_B m_e$ is the Fermi temperature. The Bohm potential can be incorporated in fluid model by taking the Madelung transformation of the Schrodinger equation [18, 27]. The Bohm potential term or Bohm-de Broglie term when added to the right hand side of Eq.(1.2), it reads

$$\mathbf{F}_Q = \frac{\hbar^2}{2m_e}\nabla\frac{\nabla^2\sqrt{n_e}}{\sqrt{n_e}}. \tag{1.8}$$

This potential explains the dispersive properties of degenerate electrons and often referred as quantum recoil force associated with the electron tunneling and the overlapping electron wave functions. In this thesis quantum effects are only due to electrons while ions are treated classically.

1.3 Quantum Plasmas

The classical plasma physics mainly deals with high temperature and low density plasma regimes. In highly dense plasma regimes like white dwarfs, where the density approaches to $10^{36}m^{-3}$, the plasma becomes degenerate and quantum effects become important. It is postulated that when the de Broglie wavelength of the plasma particles is equal to or greater than the

average distance between the particles $n^{-1/3}$ then quantum effects start playing a significant role, i.e., when

$$n\lambda_B^3 \geq 1 \tag{1.9}$$

where

$$\lambda_B = \frac{\hbar}{m_e v_{te}} \tag{1.10}$$

is the de Broglie wavelength and $v_{te} = \sqrt{\frac{k_B T_e}{m_e}}$ is the thermal velocity of electrons. The above equation shows that the quantum effects associated with electrons are more dominant than ions. Therefore, electrons are supposed degenerate and ions are classical. According to the statistical mechanics of ordinary gases, when thermal temperature is lower than the Fermi temperature then quantum effects become significant. The Fermi-Dirac distribution explains the degenerate electron gas

$$f_e\left(E\right) = \frac{1}{1 + \exp\left[\left(E - \mu_e\right)/k_B T_e\right]} \tag{1.11}$$

where E is the kinetic energy and μ_e is the chemical potential of the electrons. The Fermi temperature and Fermi energy can be defined as [66]

$$k_B T_{Fe} = E_F = \frac{\hbar^2}{2m_e}(3\pi^2)^{2/3} n^{2/3}. \tag{1.12}$$

From Eq.(1.10), we can write T_e in the form of λ_B as

$$T_e = \frac{\hbar^2}{m k_B \lambda_B^2} \tag{1.13}$$

From Eq.(1.12) and Eq.(1.13) we can get the ratio of Fermi to thermal temperature:

$$\chi = \frac{T_{Fe}}{T_e} = \frac{1}{2}(3\pi^2)^{2/3}\left(n\lambda_B^3\right)^{2/3}. \tag{1.14}$$

This equation relates the ratio χ and dimensionless parameter $n\lambda_B^3$. Thus for degenerate or quantum plasma $\chi \geq 1$.

For the plasma environments where $T_{Fe} >> T_e$, new typical space, time and velocity scales should be defined. The time scale for quantum plasma is still obtained by the inverse of the plasma frequency i.e., $\tau = \omega_p^{-1} = \sqrt{m/4\pi n e^2}$. However, the thermal velocity approaches to

zero for fully degenerate plasmas and it will be replaced by the Fermi velocity characterized by the Fermi-Dirac distribution as

$$v_F = \left(\frac{2E_F}{m_e}\right)^{1/2} = \frac{\hbar}{m_e}(3\pi^2 n)^{1/3}. \tag{1.15}$$

A typical scale length can be defined with Fermi velocity and plasma frequency:

$$\lambda_F = \frac{v_F}{\omega_p}. \tag{1.16}$$

This is the Thomas-Fermi length which defines the scale of electrostatic screening in quantum plasmas similar to the Debye length for classical plasmas.

At absolute zero $T_e \to 0$, the Fermi-Dirac distribution function (1.11) changes to a unit step function. For $\mu_e < E$, $f_e(E) = 0$ and for $\mu_e \geq E$, $f_e(E) = 1$. Thus at absolute zero the chemical potential equals to the Fermi energy

$$\mu_e = E_F \qquad \text{For} \qquad T_e = 0 \tag{1.17}$$

At low but finite thermal temperature in degenerate electron gas, chemical potential is defined as

$$\mu_e = E_F \left[1 - \frac{\pi^2}{12}\left(\frac{k_B T_e}{E_F}\right)^2\right] \qquad \text{For} \qquad 0 < T_e < T_F \tag{1.18}$$

From above equation we can see that the chemical potential is positive at low temperatures and it is negative at high temperatures. Thus the pressure of such a degenerate electron gas is given as [73]

$$P = P_F \left[1 + \frac{5}{12}\pi^2 \left(\frac{k_B T_e}{E_F}\right)^2\right] \qquad \text{For} \qquad 0 < T_e < T_F \tag{1.19}$$

where

$$P_F = \frac{2}{5} n E_F \tag{1.20}$$

1.3.1 Plasma Coupling Parameter

Energy coupling parameter of the quantum plasma or quantum coupling parameter is the ratio of interaction energy E_{int} to the average kinetic energy E_{kin} as

$$\Gamma_Q = \frac{E_{int}}{E_F} = \frac{2}{(3\pi^2)^{2/3}} \frac{4\pi e^2 m}{\hbar^2 n^{1/3}} \sim \left(\frac{1}{n\lambda_F^3}\right)^{2/3} \sim \left(\frac{\hbar\omega_p}{E_F}\right)^2 \tag{1.21}$$

For a comparison we write the classical coupling parameter:

$$\Gamma_C = \frac{E_{int}}{E_{kin}} = \frac{4\pi e^2 n^{1/3}}{k_B T} = \left(\frac{1}{n\lambda_D^3}\right)^{2/3} \tag{1.22}$$

where λ_D is the Debye length. The collisionless plasma regime where collective and mean-field effects dominate, is defined by small coupling parameters both for classical and quantum plasmas. As concern with density, it is clear from Eq.(1.21) that quantum plasma is collisionless and more collective at high densities, in contrast to the classical plasma[see Eq.(1.22)]. The last term of Eq.(1.21) has no classical parameter which defines the coupling parameter as a ratio of plasmon energy $\hbar\omega_p$ to the Fermi energy. In Eq.(1.21) the expression $\left(n\lambda_F^3\right)^{-2/3}$ is analogous to classical when we substitute $\lambda_F \rightarrow \lambda_D$. The number of particles should be large in Fermi (Debye) sphere i.e., $n\lambda_F^3 >> 1$ $\left(n\lambda_D^3 >> 1\right)$ for quantum (classical) plasmas to be collisionless and more collective.

1.3.2 Fluid Description of Spin Model

The spin property of the plasma species is the quantum mechanical effect. This effect enters into the fluid model through magnetization current and the magnetic dipole force. To derive a complete set of multi-fluid spin plasma equations we assume the electron wave function in the form $\Psi = \Psi_{(1)}\Psi_{(2)}...\Psi_{(N)}$, where N is the number of states of particles. The Pauli equation for the spin-1/2 particles in non-relativistic case is given by

$$i\hbar\frac{\partial\Psi_{(\alpha)}}{\partial t} = \left[-\frac{\hbar^2}{2m_j}\left(\nabla - \frac{iq_j}{\hbar}\mathbf{A}\right)\cdot\left(\nabla - \frac{iq_j}{\hbar}\mathbf{A}\right) - \mu_j\mathbf{B}\cdot\boldsymbol{\sigma} + q_j\phi\right]\Psi_{(\alpha)} \tag{1.23}$$

where α is for particle states, m_j is the particle mass, q_j the particle charge, $\mu_j = q_j\hbar/2m_jc$ is magnetic moment of the particle, $j = i$(ions), e (electrons), $+$(spin up electrons), $-$(spin down electrons), $\mathbf{A}$ is the vector potential, ϕ is the electrostatic potential, and $\boldsymbol{\sigma} = (\sigma_1, \sigma_2, \sigma_3)$

are the Pauli spin matrices. The explicit expressions for the Pauli spin matrices are given as:

$$\sigma_1 = \begin{pmatrix} 0 & 1 \\ 1 & 0 \end{pmatrix},\ \sigma_2 = \begin{pmatrix} 0 & -i \\ i & 0 \end{pmatrix},\ \sigma_3 = \begin{pmatrix} 1 & 0 \\ 0 & -1 \end{pmatrix}. \tag{1.24}$$

Now we introduce the decomposition of the two-component spinor $\Psi_{(\alpha)}$ carrying the spin-1/2 properties as

$$\Psi_{(\alpha)} = \sqrt{n_{(\alpha)}} \exp\left[iR_{(\alpha)}/\hbar\right] \varphi_{(\alpha)} \tag{1.25}$$

where $R_{(\alpha)}$ is the phase, $\varphi_{(\alpha)}$ is 2-spinor and $n_{(\alpha)}$ is the density. To derive the fluid momentum equation and the continuity equation, we multiply the Pauli equation (1.23) by $\Psi^{\dagger}_{(\alpha)}$, substitute the decomposition (1.25) and finally obtain [51]

$$\frac{\partial n_{(\alpha)}}{\partial t} + \nabla.\left(n_{(\alpha)}\mathbf{v}_{(\alpha)}\right) = 0 \tag{1.26}$$

and

$$\begin{aligned} m_j\left(\frac{\partial}{\partial t} + \mathbf{v}_{(\alpha)}.\nabla\right)\mathbf{v}_{(\alpha)} &= q_j\left(\mathbf{E} + \mathbf{v}_{(\alpha)}\times\mathbf{B}\right) + \frac{\hbar^2}{2m_j}\nabla\left(\frac{\nabla^2\sqrt{n_{(\alpha)}}}{\sqrt{n_{(\alpha)}}}\right) \\ &\quad + \frac{2\mu_j}{\hbar}\left(\nabla\otimes\mathbf{B}\right).\mathbf{s}_{(\alpha)} - \frac{1}{m_j n_{(\alpha)}}\nabla.\left(n_{(\alpha)}\Sigma_{(\alpha)}\right), \end{aligned} \tag{1.27}$$

where the tensor product can be written as $\left(\nabla\otimes\mathbf{B}\right).\mathbf{s}_{(\alpha)} = \nabla_a B_b s^b_{(\alpha)}$, where indices $a,\ b, ... = x, y, z$ denotes the Cartesian coordinates. Here $\mathbf{v}_{(\alpha)} = \frac{1}{m_j}\left(\nabla R_{(\alpha)} - i\hbar\varphi^{\dagger}_{(\alpha)}\nabla\varphi_{(\alpha)}\right) + \left(q_j/m_j c\right)\mathbf{A}$ is the velocity, $\mathbf{s}_{(\alpha)} = \left(\hbar/2\right)\varphi^{\dagger}_{(\alpha)}\boldsymbol{\sigma}\varphi_{(\alpha)}$ is the spin density vector which satisfies $\left|\mathbf{s}_{(\alpha)}\right| = \hbar/2$ and $\Sigma_{(\alpha)} = \left(\nabla s_{(\alpha)a}\right)\otimes\left(\nabla s^a_{(\alpha)}\right)$ is the symmetric gradient spin tensor which is the nonlinear spin correction to the classical momentum equation.

To derive the spin evolution equation, contracting Eq.(1.23) by $\Psi^{\dagger}_{(\alpha)}\boldsymbol{\sigma}$ we get

$$\left(\frac{\partial}{\partial t} + \mathbf{v}_{(\alpha)}.\nabla\right)\mathbf{s}_{(\alpha)} = -\frac{2\mu_j}{\hbar}\mathbf{B}\times\mathbf{s}_{(\alpha)} + \frac{1}{m_j n_{(\alpha)}}\mathbf{s}_{(\alpha)}\times\left[\partial_a\left(n_{(\alpha)}\partial^a\mathbf{s}_{(\alpha)}\right)\right] \tag{1.28}$$

Now we define the total number density according to

$$n_j = \sum_{(\alpha)=1}^{N} \rho_\alpha n_{(\alpha)} \tag{1.29}$$

and ensemble average of any tensorial quantity f as

$$\langle f \rangle = \sum_{(\alpha)} \rho_\alpha \left(n_{(\alpha)}/n_j \right) f \tag{1.30}$$

where ρ_α is the probability according to the wave-function $\Psi_{(\alpha)}$. Let the total fluid velocity be $\mathbf{v}_j = \left\langle \mathbf{v}_{(\alpha)} \right\rangle$ and total spin density be $\mathbf{S}_j = \left\langle \mathbf{s}_{(\alpha)} \right\rangle$, then the microscopic velocity of the species in the rest frame of the fluid will be $w_{(\alpha)} = \mathbf{v}_{(\alpha)} - \mathbf{v}_j$ such that $\left\langle w_{(\alpha)} \right\rangle = 0$ and the microscopic spin density will be $\mathbf{S}_{(\alpha)} = \mathbf{s}_{(\alpha)} - \mathbf{S}_j$ such that $\left\langle \mathbf{S}_{(\alpha)} \right\rangle = 0$.

Using the above ensemble averages in Eqs.(1.26–1.28) we get

$$\frac{\partial n_j}{\partial t} + \nabla . \left(n_j \mathbf{v}_j \right) = 0, \tag{1.31}$$

$$\begin{aligned} m_j n_j \left(\frac{\partial}{\partial t} + \mathbf{v}_j . \nabla \right) \mathbf{v}_j &= q_j n_j \left(\mathbf{E} + \mathbf{v}_j \times \mathbf{B} \right) - \nabla P_j + \frac{n_j \hbar^2}{2 m_j} \nabla \left(\frac{\nabla^2 \sqrt{n_j}}{\sqrt{n_j}} \right) \\ &+ \frac{2 n_j \mu_j}{\hbar} \left(\nabla \otimes \mathbf{B} \right) . \mathbf{S}_j, \end{aligned} \tag{1.32}$$

and

$$\left(\frac{\partial}{\partial t} + \mathbf{v}_j . \nabla \right) \mathbf{S}_j = - \frac{2 \mu_j}{\hbar} \mathbf{B} \times \mathbf{S}_j \tag{1.33}$$

In obtaining Eqs.(1.31–1.33) the last term on the right hand side of Eq.(1.27) has been neglected because of the higher order of $\hbar$ and the second term on the right hand side of Eq.(1.28) has been neglected because of $\hbar k^2 / m_e << \omega_{ce} = eB/m_e c$, c is the velocity of light in vacuum. $P_j = m_j n_j \left\langle w_\alpha^2 \right\rangle$ is the pressure. The third term on the right hand side of Eq.(1.32) is the gradient of quantum potential (or Bohm potential). The spin evolution Eq.(1.33) is used for mathematical treatment of additional spin variable $\mathbf{S}_j$. The plasma species are coupled through electromagnetic field. Let we define $\mathbf{H} = \mathbf{B} - \mathbf{M}$ where $\mathbf{M} = 2 n_j c \mu_j \mathbf{S}/\hbar$ is the magnetization

due to spin property of the plasma species. By definition, Ampere's law $\nabla \times \mathbf{H} = \frac{\mathbf{4\pi}}{\mathbf{c}}\mathbf{J} + \frac{1}{c}\partial_t \mathbf{E}$ takes the form

$$\nabla \times \mathbf{B} = \frac{4\pi}{c}\left(\mathbf{J}_q + \mathbf{J}_m\right) + \frac{1}{c}\frac{\partial \mathbf{E}}{\partial t}, \tag{1.34}$$

where $\mathbf{J}_q$ is the free current density and $\mathbf{J}_m = \nabla \times \mathbf{M}$ is the magnetization spin current density. Finally the Faraday's law

$$\nabla \times \mathbf{E} = -\frac{1}{c}\frac{\partial \mathbf{B}}{\partial t} \tag{1.35}$$

will close the system of equations. When plasma is immersed in the uniform external magnetic field then charged particles align their spin magnetic dipole moments parallel or antiparallel to external magnetic field. The spin evolution Eq.(1.33) implies that

$$\mathbf{S}_{0\pm} = \mp\frac{\hbar}{2}\widehat{\mathbf{B}} \quad \text{or} \quad |\mathbf{S}_{0\pm}| = \mp\frac{\hbar}{2} \tag{1.36}$$

where $\mathbf{S}_{0\pm}$ represents the two unperturbed spin states, spin up (parallel) and spin down (anti-parallel) to the magnetic field, respectively. In electron-ion plasma the spin effects are taken only due to electrons and ions are treated classically because ions have negligible magnetic moments due to their heavy mass. In thermodynamical equilibrium the sum and difference of unperturbed number density of the two spin populations are

$$n_{0+} + n_{0-} = n_{0e} \tag{1.37}$$

and

$$n_{0+} - n_{0-} = n_{0e} \tanh\left(\frac{\mu_B B_0}{k_B T_e}\right) \tag{1.38}$$

where n_{0+} is spin up, n_{0-} is spin down electron number density, n_{0e} is the total electron number density, T_e is the electron thermal temperature, k_B is Stefan-Boltzmann constant and $\mu_B = e\hbar/2m_e c$ is Bohar magneton.

The expression (1.38) can be derived easily by using Boltzmann statistics. According to Boltzmann statistics the number density of spin up and spin down electron population in the presence of magnetic field B_0 at any temperature T_e can be

$$n_{0+} \propto \exp\left[-E_+/k_B T_e\right] \tag{1.39}$$

and

$$n_{0-} \propto \exp\left[-E_-/k_BT_e\right] \tag{1.40}$$

where $E_+ = -\mu_B B_0$ and $E_- = \mu_B B_0$ are the potential energies also called Zeeman energies of parallel and antiparallel spin dipoles in magnetic field respectively [71]. The ratio n_{0+} to n_{0-} and ratio n_{0-} to n_{0+} can be

$$\frac{n_{0+}}{n_{0-}} = \exp\left[2\mu_B B_0/k_BT_e\right] \tag{1.41}$$

$$\frac{n_{0-}}{n_{0+}} = \exp\left[-2\mu_B B_0/k_BT_e\right] \tag{1.42}$$

Now it is possible to express n_{0+} and n_{0-} separately in term of n_{0e}. As

$$\frac{n_{0e}}{n_{0-}} = 1 + \frac{n_{0+}}{n_{0-}} \tag{1.43}$$

which finally gives

$$n_{0+} - n_{0-} = n_{0e}\frac{\exp\left[\mu_B B_0/k_BT_e\right] - \exp\left[-\mu_B B_0/k_BT_e\right]}{\exp\left[\mu_B B_0/k_BT_e\right] + \exp\left[-\mu_B B_0/k_BT_e\right]} = n_{0e}\tanh\left(\frac{\mu_B B_0}{k_BT_e}\right) \tag{1.44}$$

This expression can only be used when thermal temperature T_e is greater than the Fermi temperature $T_{Fe} = \hbar^2(3\pi^2 n_{0e})^{2/3}/2k_B m_e$. On the other hand for plasma regime where $T_{Fe} > T_e$, the unperturbed density difference of the two spin populations can be written as [61, 66]

$$n_{0+} - n_{0-} = n_{0e}\frac{3}{2}\frac{\mu_B B_0}{k_BT_{Fe}}. \tag{1.45}$$

1.4 Linearization and Fourier Decomposition

Plasma system is complex and nonlinear. It is not easy to understand the plasma system due to its non-linear behavior. The understanding of plasma dynamics becomes very easy with in the linear wave theory. In this theory we suppose that system is linearly perturbed around an equilibrium value. Here we have neglect the quadratic and higher order perturbations because the amplitude of oscillation is assumed small. In this thesis the physical quantities that are

velocity, number density, electric field, magnetic field and spin are linearized as given below

$$\mathbf{v}_j = \mathbf{v}_{1j} \tag{1.46}$$

$$n_j = n_{0j} + n_{1j} \tag{1.47}$$

$$\mathbf{B} = \mathbf{B}_0 + \mathbf{B}_1 \tag{1.48}$$

$$\mathbf{E} = \mathbf{E}_1 \tag{1.49}$$

and

$$\mathbf{S}_j = \mathbf{S}_{0j} + \mathbf{S}_{1j} \tag{1.50}$$

where the quantity with subscript 0 represents the equilibrium state and the subscript 1 shows the perturbed state. The perturbed parts of the quantities are assume to oscillate sinusoidally with $\exp[i\mathbf{k}.\mathbf{r} - i\omega t]$. The phase velocity of the wave in plasma can be calculated from the constant phase so that $(d/dt)(\mathbf{k}.\mathbf{r} - \omega t) = 0$ or

$$\mathbf{v}_\phi = \frac{\omega}{k}\widehat{\mathbf{k}}$$

This is called the phase velocity which may exceed the speed of light. It does not violate the theory of relativity because the constant phase carries no information. The modulated waves, however, can carry information and transfer energy within plasma. They move with group velocity that is less than the velocity of light,

$$v_g = \frac{d\omega}{dk}.$$

The oscillating quantities can be expressed with the product of complex amplitude and oscillating factor $\exp[i\mathbf{k}.\mathbf{r} - i\omega t]$ as

$$\mathbf{v}_1 = \widetilde{\mathbf{v}}_1 \exp[i\mathbf{k}.\mathbf{r} - i\omega t] \tag{1.51}$$

$$n_1 = \widetilde{n}_1 \exp[i\mathbf{k}.\mathbf{r} - i\omega t] \tag{1.52}$$

$$\mathbf{B}_1 = \widetilde{\mathbf{B}}_1 \exp[i\mathbf{k}.\mathbf{r} - i\omega t] \tag{1.53}$$

$$\mathbf{E}_1 = \widetilde{\mathbf{E}}_1 \exp[i\mathbf{k}.\mathbf{r} - i\omega t] \tag{1.54}$$

$$\mathbf{S}_1 = \widetilde{\mathbf{S}}_1 \exp[i\mathbf{k}.\mathbf{r} - i\omega t] \tag{1.55}$$

When we apply this sinusoidal character on a linear differential equation then differential operators are replaced with algebraic operators and hence forth the differential equations become algebraic equations. The space derivative ∇ is replaced with $i\mathbf{k}$ and the time derivative ∂_t is replaced with $-i\omega$. This decomposition of the coordinate space to the Fourier space is called the Fourier transform. With Fourier decomposition we can change signal into its constituent harmonics.

1.5 Plasma Instabilities

Plasmas are nonlinear in nature and are studied for numerous types of instability phenomena [31]. Plasma collective behavior due to long range of electromagnetic forces establishes the oscillations and instabilities. The general classification of instabilities in plasma can be divided into two categories: macroinstabilities at long wavelengths and microinstabilities at relatively shorter wavelengths.

The motion of charged particles can be controlled by the magnetic field. Therefore the instabilities in magnetized plasmas depend on the magnetic field and spatial variations of physical quantities such that number density, temperature.

1.6 Three Wave Interaction

Three wave interaction is the lowest order of wave-wave interaction in a plasma which involves either the coalescence of two waves into one, or the decay of one wave into two. This is

an efficient process to explain the non-linear emission processes which are important in both non-linear optics and non-linear plasma physics. The parametric instability can be explained quantum mechanically as decay of a pump wave photon of energy $\hbar\omega_0$ and momentum $\hbar\mathbf{k}_0$ into two quanta with energies $\hbar\omega$ and $\hbar\omega_1$ and momenta $\hbar\mathbf{k}$ and $\hbar\mathbf{k}_1$ respectively. Law of conservation of energy and momentum gives

$$\omega_0 = \omega + \omega_1 \tag{1.56}$$

and

$$\mathbf{k}_0 = \mathbf{k} + \mathbf{k}_1 \tag{1.57}$$

Classically these are the phase matching conditions for the parametric decay process. In this case, the growing waves $(\omega, \mathbf{k})$ and $(\omega_1, \mathbf{k}_1)$ are the existing linear modes of plasma. The high frequency mode $(\omega_1, \mathbf{k}_1)$ is called as sideband and $(\omega, \mathbf{k})$ act as the low frequency mode which satisfies $\omega < \omega_1, \omega_0$. In plasma, the pump drives the high frequency mode at $\omega_1 \approx \omega_0$ and there is a mismatch frequency $\omega_0 - \omega_1$. This frequency mismatch coincides with a low frequency at ω. Consequently, pump decays and two daughter waves grow.

For non-dissipative systems in homogeneous mediums three wave interaction generally is subject to Manley-Rowe symmetries. Manley-Rowe symmetry have a number of important consequences that [85, 86]:

(1)_ It expresses the conservation of energy for the harmonic generation processes in which a reduction in the photon flux at one incident beam at frequency ω_0 can lead to the generation of photon fluxes at two frequencies ω and ω_1.

(2)_When all interacting waves have positive energy, the excited daughter waves always have lower frequency than the pump wave.

(3)_The pump wave loses energy in proportion to its frequency and each of the daughter waves gain energy in direct proportion to its frequency.

(4)_It satisfies the equations (1.56–1.57) and growth rate formula for three wave interactions.

The pump may be external or internal. In the study of laser plasma interaction the high power electromagnetic wave as a pump wave interacts with plasmas either in process of stimu-

lated Raman scattering or stimulated Brillouin scattering. The Raman instability and Brillouin instability are the types of parametric instability. In Raman instability a large amplitude light wave scatters into an electron plasma wave and an electromagnetic wave, while in Brillouin instability a large amplitude light wave scatters into an ion acoustic wave and an electromagnetic wave.

In plasma nonlinear effects grow due to $\mathbf{v} \times \mathbf{B}$, pondermotive forces, nonlinear currents, velocity dependent collision frequency and change of mass due to relativistic velocities. These terms result a pump wave of large amplitude. This internal pump may be electrostatic as well as electromagnetic wave but in the present study we have taken pump wave only as an electrostatic wave. The nonlinear generation of electromagnetic waves in earth's magnetosphere has been explained by the parametric decay of upper hybrid wave into electromagnetic radiations (low frequency radio emissions) and lower hybrid wave [6]. In heating plasma experiment, the plasma is exposed to a high power electromagnetic wave. The wave is either absorbed through Landau damping or converted into another mode by resonance with a local eigenfrequency. Near the resonance, the wave gets high amplitude which becomes the internal pump wave and may decay into other modes.

Chapter 2

Motivations

The parametric decay instability problem has attained a great deal of interest over the years and has been investigated in detail for the wave-wave interactions in plasmas [3]–[14]. This field has further flourished after the theoretical explanation of the generation of electromagnetic waves in the Earth's magnetosphere by analyzing the Earth-orbiting satellites data [64, 74]. In this data analysis electromagnetic narrow band frequency slightly greater than the electron plasma frequency [77]–[80], the electrostatic oscillations above upper-hybrid frequency [79]–[83] and the lower-hybrid frequency [75, 84] were found. Melrose emphasized that the generation of electromagnetic wave in the Earth's magnetosphere is result of coalescence of upper hybrid turbulence with ion cyclotron irregularities [76]. It thus seems that a nonlinear wave-wave interaction phenomenon might be active in the radiation source regions of Earth's magnetosphere [75]–[77]. Finally, in 1984 Murtaza and Shukla [6] proposed that the parametric instability of a perpendicularly propagating electrostatic pump near the upper-hybrid frequency could possibly be the source to excite the radiations (O-mode, left-hand circularly polarized wave, X-mode). Later some authors investigated the parametric interaction of waves in different plasma environment e.g., dusty plasmas [12] and quantum plasmas [14, 16]. The above mentioned applications of the parametric instability motivated me to study three wave interactions in various plasma regimes.

In a parametric instability, a pump wave excites sidebands and low frequency fluctuations. Such a three-wave interaction phenomenon has significant applications in laser fusion experiments, ionospheric modification experiments and pulsar electrodynamics [8], [38]–[43]. Among

the parametric processes, stimulated Raman scattering, stimulated Brillouin scattering and the two-plasmon decay instability have been extensively studied to explain the laser plasma interaction phenomena [4, 9, 10].

Yu and Shukla [44] illustrated the nonlinear coupling of upper-hybrid (UH) waves with low-frequency ion-cyclotron (IC) waves and obtained near-sonic UH cusped envelope solitons in a classical magneto-plasma. Dysthe et al., [45] studied the nonlinear interaction between a high frequency oblique Langmuir wave, which propagates at an arbitrary angle to a weak magnetic field, and a low frequency ion-cyclotron or ion-sound perturbation. Kaufman and Stenflo [69] analyzed the non-linear interaction between the UH waves and the magneto-sonic modes, and showed how the UH solitons could be formed.

Quantum plasma [18]–[35] physics has received great attention in the last decade mainly due to its possible applications in metallic nano-structures [36], quantum wells [34], ultracold plasmas [32, 33], microelectronic components [46], dense astrophysical systems (in particular, white dwarf and neutron star environments) [35], intense laser matter interaction experiments [37]–[45] and semiconductor physics [46]. The quantum effects are important in low temperature dense plasmas. The list of quantum mechanical effects in a fluid picture, in general, includes the dispersive particle properties accounted for the Bohm potential [16]–[20], [22, 23, 26], the zero temperature Fermi pressure [18, 19, 22, 26] and certain quantum electrodynamical effects. When the thermal de Broglie wavelength of the charged particles is equal to or larger than the average interparticle distance then quantum mechanical effects play an important role in the dynamics of the charged particles [18]. Recently, study of three-wave interaction problem also gained momentum in quantum plasmas [14]–[16], [57]. The analysis of plasma instabilities in quantum plasmas [14, 16], [26]–[31], [57] has shown that the quantum effects can significantly influence the nature of instabilities.

Iannuzzi first time discussed the electron spin resonance in gaseous plasmas [50]. It has been emphasized that the paramagnetic resonance in the gaseous plasma might be important for measuring the plasma density with a precision much greater than that of the conventional techniques. In 2007, Brodin and Marklund have derived spin magnetohydrodynamic model [51] and observed spin solitons in magnetized pair plasmas [52]. After that, so called spin plasmas in which the spin properties of electrons are taken into account, have received great attention

[50]–[63]. When we talk about the gyration of the plasma particles, the plasmas are diamagnetic [1] but spin of the charged particles is the intrinsic property which acts paramagnetically in magnetized plasmas and hence strengthen the external magnetic field. Very recently, Hussain et al., discussed the kinetic Alfven wave in spin quantum plasma and investigated that the electron spin effects suppresses the Alfven frequency [60]. Effects of spin quantum force have been studied in different plasma regime such as in classical plasmas [55], in quantum plasmas [62], in semi-relativistic plasmas [56] and in the relativistic plasma regime [59].

It was recently shown that even for high temperature plasmas, quantum features due to intrinsic magnetic moment of the electrons [55] become noticeable and their spin effects [50]–[63] in plasmas are found to be somewhat different from those of nonspin [18]–[35] quantum effects in plasmas.

2.0.1 Layout of thesis

In chapter 3 we study the parametric decay of upper hybrid wave into O-mode and shear Alfven wave in homogenous classical electron-ion mageto-plasma. Intrinsic property of electron i.e., spin, is included. Spin fluid model has been used to investigate the spin effect on the growth rate of the parametric decay instability. Results are applied in fusion plasma environment.

In chapter 4 we investigate the three wave interaction in spin quantum plasma. Here Langmuir wave as a pump wave decays parametrically into left hand circular polarized wave and low frequency shear Alfven wave in spin degenerate magnetized electron-ion plasma. Incorporating the spin of electron we use spin quantum hydrodynamic model to calculate the nonlinear dispersion relation and growth rate of the parametric instability in degenerate magneto-plasma. It is shown that spin effect decreases the growth rate which is in favor of the stability of plasma environments. Growth rate is plotted of the dense astrophysical environments.

In chapter 5 we examine the parametric decay of Langmuir wave into left hand circular polarized wave and shear Alfven wave in highly dense (quantum) and low dense (classical) magneto-plasma. Quantum magneto-hydrodynamic model has been used to calculate the linear and nonlinear functions for plasma species for three wave interaction. Nonlinear dispersion relations and growth rates are derived for both degenerate and non-degenerate plasmas. The growth rate for a degenerate magneto-plasma has been plotted for dense astrophysical envi-

ronments like pulsar while for non-degenerate magneto-plasma we have selected the Earth's magnetosphere. It is noticed that growth rate as a function of density in the high density degenerate magneto-plasma increases exponentially while in the low density classical case it increases logarithmically. Summary and discussion of this dissertation is given in chapter 6.

Chapter 3

Spin Effect on Parametric Interactions of Waves in Magneto-plasmas

The parametric decay instability of upper hybrid wave into low-frequency electromagnetic Shear Alfven wave and Ordinary mode radiation has been investigated in electron-ion magneto-plasmas. To handle the spin properties of electrons, the fluid model has been used to investigate the linear and nonlinear response of the plasma species for three-wave coupling in a magneto-plasma. It is shown that the spin properties of electrons have considerable effect on the growth rate of three-wave interactions even in classical plasma regime [65].

3.1 Introduction

In this chapter, we study the three wave interaction in nonrelativistic classical magnetized plasma, in which upper hybrid wave (UHW) as a pump decays parametrically into a low frequency electromagnetic shear Alfven wave (SAW) and an ordinary mode radiations (O-mode). Here a finite-amplitude electrostatic pump at frequency ω_0 propagates linearly in xz-plane at small angle with the positive x-direction. This pump drives the O-mode radiation at $\omega_r \approx \omega_0$, and then there is a frequency mismatch $\omega_0 - \omega_r$. This frequency mismatch coincides with a low frequency SAW at ω_A. In this process when scattered sideband O-mode at (ω_r, k_r) propagating

exactly perpendicular to the external magnetic field, beats with the pump at (ω_0, k_0), generates a nonlinear current which becomes the source to enhance the SAW at (ω_A, k_A). SAW propagates obliquely to z-axis. The excited SAW interacts with the pump wave hence again generating a nonlinear current which becomes the source of the modified (or amplified) scattered sideband O-mode radiation (See Fig.3-1).

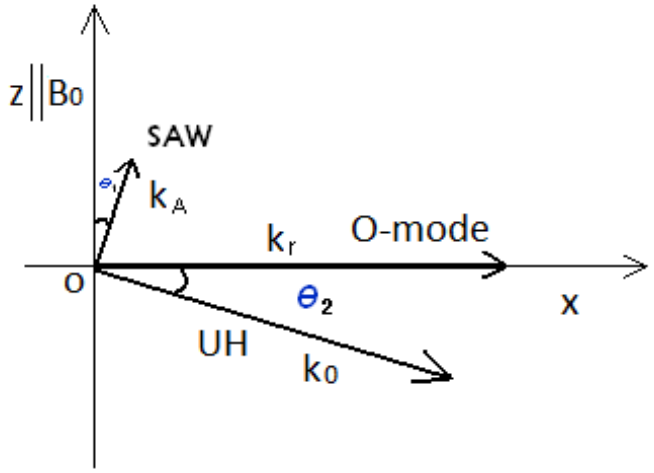

Figure 3-1: Schematic diagram of propagation of UH, O-mode and SAW in xz-plane.

These three waves satisfy the following phase matching conditions [4]

$$\omega_0 = \omega_r + \omega_A \tag{3.1}$$

$$\mathbf{k}_0 = \mathbf{k}_r - \mathbf{k}_A \tag{3.2}$$

In this chapter our special focus is on the spin property of electrons. How does the spin property of electrons influence the growth rate of the above mentioned three wave interaction problem? Spin plays a vital role on exposing the plasma to an external magnetic field, later interacts with the magnetization in the plasma due to the electron spin. In magnetized plasmas, electrons align their spin magnetic dipole moments parallel or anti parallel to the external magnetic field. Then spin up and spin down electrons are considered as two different fluids. According to the thermodynamical equilibrium in the presence of ambient magnetic field the

spin up population is greater than the spin down population as [55]

$$n_{0+} - n_{0-} = n_{0e} \tanh\left(\frac{\mu_B B_0}{k_B T_e}\right). \tag{3.3}$$

Hence, the resulting spin magnetization enhances the strength of external magnetic field. This increase of the external magnetic field makes the plasma stable and hence decreases the growth rate of parametric instability.

Employing fluid model, in Section 3.2, we solve the fluid equations of homogeneous magneto-plasmas in order to achieve the nonlinear current densities, later are used to derive the nonlinear dispersion relations for O-mode and Shear Alfvén waves. Finally, the nonlinear dispersion relation for the three wave interaction is calculated in Section 3.3. In Section 3.4, growth rate of the three wave parametric instability is obtained. The graphical representation of the growth rate is given for some typical parameters in Section 3.5. A brief discussion of the result is presented in Section 3.6.

3.2 Mathematical Model

The nonlinear interaction of waves in a magnetized spin plasma is governed by the following fluid equations, the Maxwell equations and the spin evolution equation [53, 63]

$$\frac{\partial \mathbf{v}_j}{\partial t} = \frac{q_j}{m_j}\mathbf{E} + \mathbf{v}_j \times \omega_{cj}\hat{\mathbf{z}} - \frac{\nabla P_j}{m_j n_{0j}} + \frac{2\mu_j}{\hbar m_j} S_j^a \nabla B_a \tag{3.4}$$

$$\frac{\partial n_j}{\partial t} + \nabla.(n_j \mathbf{v}_j) = 0 \tag{3.5}$$

$$\boldsymbol{\nabla} \times \mathbf{E} = -\frac{1}{c}\frac{\partial \mathbf{B}}{\partial t} \tag{3.6}$$

$$\boldsymbol{\nabla} \times \mathbf{B} = \frac{4\pi}{c}\mathbf{J} + \frac{1}{c}\frac{\partial \mathbf{E}}{\partial t} \tag{3.7}$$

$$\boldsymbol{\nabla}.\mathbf{E} = 4\pi \sum_j q_j n_j \tag{3.8}$$

$$\left(\frac{\partial}{\partial t} + \mathbf{v}_j.\nabla\right)\mathbf{S}_j = \frac{2\mu_j}{\hbar}\mathbf{S}_j \times \mathbf{B} \tag{3.9}$$

where B is total magnetic field, a = (x, y, z) such that the spin term $S_j^a \nabla B_a$ can be expanded in the form of $S_j^x \nabla B_x + S_j^y \nabla B_y + S_j^z \nabla B_z$, $j = i$ (ions), e (electrons), + (spin up electrons), − (spin down electrons), $P_j = \gamma n_j k_B T_j$ is thermal pressure, $\omega_{cj} = q_j B_0 / m_j c$ is the cyclotron frequency, c is the speed of light in a vacuum, m_j, q_j and n_{0j}^0 are the mass, charge and equilibrium number density of jth species in plasmas; here $q_e = -e$, $q_i = +e$ with e being the magnitude of electronic charge. Note that apart from usual equations (3.4–3.8), we now have an additional equation - so called spin evolution equation - for mathematical treatment of additional spin variable S_j.

The current density in Eq.(3.7) for spin plasmas is due to charge current density J_q and magnetization current density J_m

$$\mathbf{J} = \mathbf{J}^L + \mathbf{J}^{NL} \tag{3.10}$$

$$\mathbf{J^L} = \mathbf{J}_q + \mathbf{J}_m, \qquad \mathbf{J}_q = \sum_j q_j n_j \mathbf{v}_j \tag{3.11}$$

and

$$\mathbf{J}_m = \sum_j \nabla \times \mathbf{M}_j = \sum_j \nabla \times \frac{2\mu_j n_j}{\hbar} \mathbf{S}_j \tag{3.12}$$

For three wave interaction problem we can decompose all the physical quantities in the following manner:

$$n_j = n_{0j} + n_{1j}^0 + n_{1j}^A, \qquad \mathbf{v}_j = \mathbf{v}_j^0 + \mathbf{v}_j^r + \mathbf{v}_j^A \tag{3.13}$$

$$\mathbf{E} = \mathbf{E}_0 + \mathbf{E}_r + \mathbf{E}_A \tag{3.14}$$

where the superscripts 0, r and A in Eq.(3.13) and subscripts 0, r and A in Eq.(3.14) represent the corresponding perturbed quantities associated with the pump wave, O-mode radiation and SAW respectively. The density perturbation n_{1j}^r is zero in the field of O-mode. All the perturbed physical quantities behave sinusoidally.

3.2.1 Upper Hybrid Wave

Let the pump wave propagates in infinitely extended homogeneous non-relativistic and non-degenerate plasma in xz-plane at small angle with the positive x-direction. The plasma consists of electrons and ions in the presence of static ambient/external magnetic field $B_0 \widehat{z}$. The electric field of the pump wave is taken as

$$\mathbf{E}_0 = (\hat{x}E_{0x} + \hat{z}E_{0z})\exp[-i(\omega_0 t - \mathbf{k_0}.\mathbf{r})] + c.c. \tag{3.15}$$

The angular frequency ω_0 and the wave vector k_0 of the UHW are related by the following dispersion relation [5]–[7],

$$\omega_0^2 = \omega_{pe}^2 + \omega_{ce}^2 + \frac{3k_{0x}^2 v_{te}^2 \omega_{pe}^2}{\omega_{pe}^2 - 3\omega_{ce}^2} - \frac{k_{0z}^2}{k_{0x}^2}\frac{\omega_{ce}^2\omega_{pe}^2}{(\omega_{pe}^2 + \omega_{ce}^2)} \tag{3.16}$$

Here, $\omega_{pe} = \sqrt{4\pi n_{oe}e^2/m_e}$ is the electron plasma frequency, $\omega_{ce} = eB_0/m_e c$ is electron gyrofrequency, v_{te} is the electron thermal velocity and $k_{0z}\,(k_{0x})$ is the component of wave vector parallel (perpendicular) to the ambient magnetic field $B_0\widehat{z}$.

As UHW is high frequency wave therefore it will excite lighter particles i.e., electrons. To calculate the perturbed number densities and velocities of plasma species in parametric instability phenomenon, we first linearize the Eqs.(3.4–3.9) and then use sinusoidal character for perturbed quantities. Thus x- and z-components of the linear velocity of electrons due to pump wave can be obtained from Eq.(3.4) and Eq.(3.5) as

$$v_{xe}^0 = -\frac{ie\omega_0 E_{0x}}{m_e(\omega_0^2 G_0 - \omega_{ce}^2)} - \frac{iek_{0x}k_{0z}v_{te}^2 E_{0z}}{m_e\omega_0 F_0(\omega_0^2 G_0 - \omega_{ce}^2)} \tag{3.17}$$

and

$$v_{ze}^0 = \frac{-ie}{m_e\omega_0 F_0}\left\{\frac{k_{0x}k_{0z}v_{te}^2}{(\omega_0^2 G_0 - \omega_{ce}^2)}E_{0x} + \left(1 + \frac{k_{0x}^2 k_{0z}^2 v_{te}^4}{\omega_0^2 F_0(\omega_0^2 G_0 - \omega_{ce}^2)}\right)E_{0z}\right\} \tag{3.18}$$

where

$$F_0 = 1 - \frac{k_{0z}^2 v_{te}^2}{\omega_0^2}$$

and

$$G_0 = \frac{\omega_0^2 - k_0^2 v_{te}^2}{\omega_0^2 - k_{0z}^2 v_{te}^2}$$

For electrostatic pump we use $E_{0x} = -ik_{0x}\phi_0$ and $E_{0z} = -ik_{0z}\phi_0$, ϕ_0 is the potential and high frequency condition $\omega_0^2 > (k_{0z}^2 v_{te}^2)$, then above Eqs.(3.17 and 3.18) reduce to

$$v_{xe}^0 = -\frac{e\omega_0 k_{0x}\phi_0}{m_e(\omega_0^2 G_0 - \omega_{ce}^2)} \tag{3.19}$$

and

$$v_{ze}^{0} = -\frac{ek_{0z}}{m_e\omega_0}\left\{1 + \frac{k_{0x}^2 v_{te}^2}{\omega_0^2 G_0 - \omega_{ce}^2}\right\}\phi_0 \tag{3.20}$$

where $G_0 = 1 - (k_{0x}^2 v_{te}^2)/\omega_0^2$.

From the equation of continuity, the first perturbation in electron number density n_{1e}^0, due to the pump UHW, is obtained as

$$n_{1e}^0 = \frac{n_{0e}}{\omega_0}\left(k_{0x}v_{xe}^0 + k_{0z}v_{ze}^0\right) \tag{3.21}$$

Using values of v_{xe}^0 and v_{ze}^0 from Eq.(3.19) and Eq.(3.20) accordingly into the above equation we obtain

$$n_{1e}^0 = -\frac{en_{0e}}{m_e}\left\{\frac{k_{0z}^2}{\omega_0^2} + \frac{k_{0x}^2}{\omega_0^2 G_0 - \omega_{ce}^2}\right\}\phi_0, \tag{3.22}$$

We can see there is no contribution of the spin in the perturbed velocities and number density of electrons for electrostatic UH wave.

3.2.2 O-mode

The electromagnetic sideband O-mode at (ω_r, k_r) propagates exactly perpendicular to the external magnetic field has an electric and magnetic field respectively

$$\mathbf{E}_r = \hat{\mathbf{E}}_r exp[-i(\omega_r t - k_{rx}x)] \tag{3.23}$$

$$\mathbf{B} = \frac{\mathbf{k}_r \times \mathbf{E}_r}{c\omega_r} \tag{3.24}$$

From the Maxwell's equations, Eqs.(3.6 and 3.7), we get the wave equation of electromagnetic O-mode propagating along x-direction with electric field $\mathbf{E}_r \| \mathbf{B}_0$

$$(\omega_r^2 - \omega_{pe}^2 - c^2k_r^2)E_{rz} + i4\pi\omega_r J_{mz} = -i4\pi\omega_r J_{rz}^{NL} \tag{3.25}$$

where,

$$J_{rz}^{NL} = -e(n_{1e}^{A*}v_{ze}^0 + n_{1e}^0 v_{ze}^{A*}) \tag{3.26}$$

is the second ordered nonlinear current density due to coupling of UHW and low frequency SAW which becomes the source of the modified (or amplified) O-mode radiation.

The v_{ze}^0, n_{1e}^0 are linear velocity component and perturbed number density of electrons due to electrostatic high frequency pump wave and v_{ze}^A, n_{1e}^A are for electromagnetic low frequency viz., Shear Alfvén wave respectively. The symbol asterisk is for complex conjugate. The velocity of the electrons in the field of O-mode radiation can be obtained from Eq.(3.4) as

$$v_{ze}^r = -\frac{ie}{m_e\omega_r}E_{rz} \tag{3.27}$$

The electrons have two types of spin, that is, spin up and spin down. The electrons with spin up and down are taken as two fluids which behave differently. The z-component of magnetization current density which represents two types of spin density of electrons is defined as [55],

$$J_{mz} = ik_{rx}(M_{+y} + M_{-y}), \tag{3.28}$$

where the up and down (M_{+y}, M_{-y}) magnetization densities are

$$M_{+y} = -\frac{2c\mu_B n_{0+} S_{1+}^y}{\hbar} \tag{3.29}$$

and

$$M_{-y} = -\frac{2c\mu_B n_{0-} S_{1-}^y}{\hbar} \tag{3.30}$$

Here, S_{1+}^y and S_{1-}^y are the y-components of the spin of electrons for up and down populations respectively. We can calculate the spin of electrons from Eq.(3.6) and Eq.(3.9). First we linearize the Eq.(3.9) as

$$\partial_t \mathbf{S}_1 = \frac{2\mu_e}{\hbar}\mathbf{S}_1 \times \mathbf{B}_0 + \frac{2\mu_e}{\hbar}\mathbf{S}_0 \times \mathbf{B}_1 \tag{3.31}$$

Taking time derivative of the above equation we get

$$\partial_t^2 \mathbf{S}_1 = \frac{2\mu_e}{\hbar}\partial_t\mathbf{S}_1 \times \mathbf{B}_0 + \frac{2\mu_e}{\hbar}\mathbf{S}_0 \times \partial_t\mathbf{B}_1 \tag{3.32}$$

Using $\partial_t \mathbf{B}_1 = -c\boldsymbol{\nabla} \times \mathbf{E}_1$ from Eq.(3.6) into the Eq.(3.32) and applying Fourier decomposition

we obtain

$$\mathbf{S}_1 = -\frac{2i\mu_B}{\hbar\omega}\mathbf{S}_1 \times \mathbf{B}_0 - \frac{2i\mu_B c}{\hbar\omega^2}(\mathbf{S}_0.\mathbf{E}_1)\mathbf{k} + \frac{2i\mu_B c}{\hbar\omega^2}(\mathbf{k}.\mathbf{S}_0)\mathbf{E}_1. \tag{3.33}$$

The y-components of perturbed spin vector for spin up and spin down electrons in the field of O-mode are

$$S^y_{1+} = \frac{4\mu_B^2 cB_0 k_{rx}}{\hbar^2\omega_r(\omega_r^2 - \omega_{cg}^2)} S^z_{0+} E_{rz}, \tag{3.34}$$

and

$$S^y_{1-} = \frac{4\mu_B^2 cB_0 k_{rx}}{\hbar^2\omega_r(\omega_r^2 - \omega_{cg}^2)} S^z_{0-} E_{rz}, \tag{3.35}$$

where $\omega_{cg}^2 = 4\mu_B^2 B_0^2/\hbar^2 \approx \omega_{ce}^2$ is the characteristic spin precession frequency and $S^z_{0+} = -\hbar/2$ and $S^z_{0-} = +\hbar/2$ are the z-components for the unperturbed spin up and spin down electrons respectively. In the presence of magnetic field in z-direction and if there is no spin perturbation then electrons align themselves parallel or anti parallel to the magnetic field and the unperturbed components perpendicular to the magnetic field are zero i.e., $S^x_{0+} = S^x_{0-} = S^y_{0+} = S^y_{0-} = 0$, and z-components are $S^z_{0+} = -\hbar/2$ and $S^z_{0-} = +\hbar/2$.

Substituting the values of S^y_{1+} and S^y_{1-} from Eq.(3.34) and Eq.(3.35) into Eq.(3.29) and Eq.(3.30) respectively

$$M_{+y} = \frac{4\mu_B^3 c^2 B_0 k_{rx}}{\hbar^2\omega_r(\omega_r^2 - \omega_{cg}^2)} n_{0+} E_{rz} \tag{3.36}$$

and

$$M_{-y} = -\frac{4\mu_B^3 c^2 B_0 k_{rx}}{\hbar^2\omega_r(\omega_r^2 - \omega_{cg}^2)} n_{0-} E_{rz} \tag{3.37}$$

Putting above values of M_{+y} and M_{-y} in Eq.(3.28) we get the magnetization current density J_{mz} as

$$J_{mz} = i\frac{4\mu_B^3 c^2 B_0 k_{rx}^2}{\hbar^2\omega_r(\omega_r^2 - \omega_{cg}^2)} \left(n_{0+} - n_{0-}\right) E_{rz} \tag{3.38}$$

Using this value of J_{mz} into the Eq.(3.25) we get

$$(\omega_r^2 - \omega_{pe}^2 - c^2 k_r^2)E_{rz} - \frac{16\pi\mu_B^3 c^2 k_{rx}^2 B_0}{\hbar^2(\omega_r^2 - \omega_{cg}^2)}(n_{0+} - n_{0-})E_{rz} = i4\pi\omega_r J_{rz}^{NL} \tag{3.39}$$

The unperturbed density difference of the two spin populations $(n_{0+} - n_{0-})$ in the thermo-

dynamical equilibrium is given from Eq.(3.3). Hence, the wave equation of O-mode with spin population is

$$\left\{\omega_r^2-\omega_{pe}^2-c^2k_r^2-\frac{\omega_{pe}^2k_{rx}^2\mu_B B_0}{m_e(\omega_r^2-\omega_{ce}^2)}\tanh\left(\frac{\mu_B B_0}{k_B T_e}\right)\right\}E_{rz}=i4\pi\omega_r J_{rz}^{NL}. \tag{3.40}$$

The L.H.S of the above equation is the spin modified linear dispersion relation of O-mode and R.H.S is the source to generate the O-mode in the three wave interaction phenomenon.

3.2.3 Shear Alfven Wave

The response of the plasma particles due to SAW in this three-wave parametric process, in the presence of the ambient magnetic field B_0, is governed by the Eq.(3.6) and Eq.(3.7) with subscript and superscript A for shear Alfvén wave. The equation of electromagnetic wave (SAW) is

$$(\omega_A^2-c^2k_A^2)\mathbf{E}_A+c^2(\mathbf{k}_A.\mathbf{E}_A)\mathbf{k}_A-i4\pi e\omega_A n_{0e}\mathbf{v}_e^A+i4\pi e\omega_A n_{0i}\mathbf{v}_i^A+i4\pi\omega_A\mathbf{J}_m^A=-i4\pi\omega_A\mathbf{J}_A^{NL} \tag{3.41}$$

where

$$\mathbf{J}_m^A=i\mathbf{k}_A\times(\mathbf{M}_+ + \mathbf{M}_-) \tag{3.42}$$

is the magnetization current density due to the field of SAW and

$$\mathbf{J}_A^{NL}=-e(n_{1e}^0\mathbf{v}_e^{r*}+n_e^{r*}\mathbf{v}_e^0) \tag{3.43}$$

is the nonlinear current density being generated by the beating of the pump wave and O-mode. This nonlinear current provides the energy to SAW for amplification. For low frequency electromagnetic wave, the electrons are inertia less ($\omega_{ce}^2 \gg \omega_A^2$), $k_{Az} \gg k_{Ax}$, $E_{Ax} \gg E_{Az}$ and $k_{Az}^2v_{ti}^2 < \omega_A^2 < \omega_{ci}^2$, $k_{Az}^2v_{te}^2$. Here v_{ti} is the ion thermal velocity. Kinetic Alfven waves [47]–[49] arise in a low-β ($m_e/m_i < \beta = 8\pi n_{0e}k_BT_e/B_0^2 < 1$) plasma propagating in xz-plane and making a small angle with $\mathbf{B}_0\|\widehat{z}$. For these conditions, the x- and z-components of the Eq.(3.41) are

$$(\omega_A^2-c^2k_{Az}^2)E_{Ax}-i4\pi e\omega_A n_{0e}v_{xe}^A+i4\pi e\omega_A n_{0i}v_{xi}^A+i4\pi\omega_A J_{mx}^A=-i4\pi\omega_A J_{Ax}^{NL}, \tag{3.44}$$

and

$$\omega_A^2 E_{Az} + c^2 k_{Ax} k_{Az} E_{Ax} - i4\pi e\omega_A n_{0e} v_{ze}^A + i4\pi e\omega_A n_{0i} v_{zi}^A + i4\pi\omega_A J_{mz}^A = -i4\pi\omega_A J_{Az}^{NL}, \quad (3.45)$$

where

$$J_{mx}^A = -ik_{Az}(M_{+y} + M_{-y}), \quad (3.46)$$

$$J_{mz}^A = ik_{Ax}(M_{+y} + M_{-y}), \quad (3.47)$$

$$J_{Ax}^{NL} = -e(n_{1e}^0 v_{ex}^{r*} + n_e^{r*} v_{ex}^0), \quad (3.48)$$

and

$$J_{Az}^{NL} = -e(n_{1e}^0 v_{ez}^{r*} + n_e^{r*} v_{ez}^0). \quad (3.49)$$

As $v_{ex}^r = 0$ and $n_{1e}^r = 0$, because there is no perturbation in number density of electrons due the pure transverse O-mode then above Eqs.(3.48) and (3.49) reduce to

$$J_{Ax}^{NL} = 0, \quad (3.50)$$

and

$$J_{Az}^{NL} = -en_{1e}^0 v_{ez}^{r*}. \quad (3.51)$$

The velocity components of species can be found out from Eq.(3.4) for Shear Alfvén wave,

$$v_{xe}^A \simeq 0, \quad (3.52)$$

$$v_{ze}^A = ieE_{Az}\frac{\omega_A}{k_{Az}^2 k_B T_e}, \quad (3.53)$$

similarly

$$v_{xi}^A = -\frac{iek_{Ax}k_{Az}v_{ti}^2 E_{Az}}{\omega_{ci}^2\omega_A m_i} - \frac{ie\omega_A E_{Ax}}{\omega_{ci}^2 m_i}, \quad (3.54)$$

$$v_{zi}^A = -\frac{iek_{Ax}k_{Az}v_{ti}^2 E_{Ax}}{\omega_{ci}^2\omega_A m_i} + \frac{ieE_{Az}}{\omega_A m_i}. \quad (3.55)$$

From equation of continuity, the perturbed number density of electrons is

$$n_{1e}^{A} = \frac{n_{0e}}{\omega_A}\left(k_{Ax}v_{xe}^{A} + k_{Az}v_{ze}^{A}\right). \tag{3.56}$$

Using values of v_{xe}^{A} and v_{ze}^{A} from Eqs.(3.52 and 3.53) into the above equation we get

$$n_{1e}^{A} = ien_{0e}\frac{E_{Az}}{k_{Az}k_B T_e} \tag{3.57}$$

In order to calculate the magnetization current densities, we first write the y-components of the spin vector density from Eq.(3.33) in the field of SAW for both spin up and spin down electrons as given below

$$S_{1+}^{y} = +\frac{c\hbar k_{Ax}}{2\omega_A B_0}E_{Az} - \frac{c\hbar k_{Az}}{2\omega_A B_0}E_{Ax} \tag{3.58}$$

and

$$S_{1-}^{y} = -\frac{c\hbar k_{Ax}}{2\omega_A B_0}E_{Az} + \frac{c\hbar k_{Az}}{2\omega_A B_0}E_{Ax} \tag{3.59}$$

here $\omega_{cg}^2 \gg \omega_A^2$, $S_{0+}^{z} = -\frac{\hbar}{2}$ and $S_{0-}^{z} = +\frac{\hbar}{2}$ has been used.

Putting these values of S_{1+}^{y} and S_{1-}^{y} into Eq.(3.29) and Eq.(3.30) we get the spin magnetization

$$M_{+y} = -\frac{c^2\mu_B k_{Ax}}{\omega_A B_0}n_{0+}E_{Az} + \frac{c^2\mu_B k_{Az}}{\omega_A B_0}n_{0+}E_{Ax}, \tag{3.60}$$

and

$$M_{-y} = \frac{c^2\mu_B k_{Ax}}{\omega_A B_0}n_{0-}E_{Az} - \frac{c^2\mu_B k_{Az}}{\omega_A B_0}n_{0-}E_{Ax}. \tag{3.61}$$

After substituting M_{+y} from Eq.(3.60) and M_{-y} from Eq.(3.61) into Eqs.(3.46 and 3.47) we obtain the x- and z-components of the magnetization current densities as

$$J_{mx}^{A} = -ik_{Az}\frac{c^2\mu_B}{\omega_A B_0}\left(k_{Az}E_{Ax} - k_{Ax}E_{Az}\right)\left(n_{0+} - n_{0-}\right), \tag{3.62}$$

and

$$J_{mz}^{A} = ik_{Ax}\frac{c^2\mu_B}{\omega_A B_0}\left(k_{Az}E_{Ax} - k_{Ax}E_{Az}\right)\left(n_{0+} - n_{0-}\right). \tag{3.63}$$

Substituting the Eqs.(3.50, 3.52, 3.54 and 3.62) into Eq.(3.44) we get

$$\begin{aligned}\left(\omega_A^2 - c^2 k_{Ax}k_{Az}(1-S_p) + \frac{\omega_{pi}^2\omega_A^2}{\omega_{ci}^2}\right) E_{Ax} \\ + \left(\frac{\omega_{pi}^2}{\omega_{ci}^2}k_{Ax}k_{Az}v_{ti}^2 - c^2 k_{Ax}k_{Az}S_p\right) E_{Az} = 0,\end{aligned} \tag{3.64}$$

and substituting the Eqs.(3.53, 3.55 and 3.63) into Eq.(3.45) we get

$$\begin{aligned}\left(c^2 k_{Ax}k_{Az}(1-S_p) + \frac{\omega_{pi}^2}{\omega_{ci}^2}k_{Ax}k_{Az}v_{ti}^2\right) E_{Ax} \\ + \left(\frac{\omega_A^2}{k_{Az}^2\lambda_{De}^2} - \omega_{pi}^2 + c^2 k_{Ax}^2 S_p\right) E_{Az} = -i4\pi\omega_A J_{Az}^{NL}.\end{aligned} \tag{3.65}$$

Here $\lambda_{De}^2 = \frac{k_B T_e}{4\pi e^2 n_{0e}}$, $k_{Az}^2\lambda_{De}^2 \ll 1$ and $S_p = \frac{4\pi n_{0e}\mu_B}{B_0} tanh\left(\frac{\mu_B B_0}{k_B T_e}\right)$.

Eliminating E_{Ax} from Eq.(3.64, 3.65) we get

$$\begin{aligned}\left[\frac{\omega_A^2}{k_{Az}^2\lambda_{De}^2} - \omega_{pi}^2 + c^2 k_{Ax}^2 S_p - c^2 k_{Ax}^2 k_{Az}^2\left(1 - S_p + \frac{v_{ti}^2}{v_A^2}\right)\frac{\left(v_{ti}^2 - v_A^2 S_p\right)}{\left(\omega_A^2 - v_A^2 k_{Az}^2(1-S_p)\right)}\right] E_{Az} \\ = -i4\pi\omega_A J_{Az}^{NL}.\end{aligned} \tag{3.66}$$

Here, $v_A = \frac{B_0}{\sqrt{4\pi n_{0i} m_i}}$ is Alfv'en speed. This is the nonlinear dispersion relation of SAW. The L.H.S of the above equation is the spin modified linear dispersion relation of SAW and R.H.S is the source to amplify the SAW in the three wave interaction phenomenon.

3.3 Nonlinear Dispersion Relation

In order to find the nonlinear dispersion relation we first calculate the nonlinear current densities J_{rz}^{NL} and J_{Az}^{NL}. Now using the values of v_{ze}^0, n_{1e}^0, v_{ze}^A and n_{1e}^A, from Eqs.(3.20, 3.22, 3.53 and 3.57) into Eq.(3.26) respectively we obtain

$$J_{rz}^{NL} = \frac{i\omega_{pe}^2 e\phi_0}{4\pi k_{Az}k_B T_e}\left\{\frac{k_{0z}}{\omega_0}\left(1 + \frac{k_{0z}}{k_{Az}}\frac{\omega_A}{\omega_0}\right) + \frac{\omega_A}{k_{Az}}\left(1 + \frac{k_{Az}k_{0z}}{\omega_0\omega_A}v_{te}^2\right)\frac{k_{0x}^2}{\omega_0^2 G_0 - \omega_{ce}^2}\right\} E_{Az}^* \tag{3.67}$$

and putting n_{1e}^0 and v_{ze}^r from Eq.(3.22) and Eq.(3.27) into Eq.(3.51) respectively we get

$$J_{Az}^{NL} = \frac{ie\omega_{pe}^2\phi_0}{4\pi m_e\omega_r}\left\{\frac{k_{0z}^2}{\omega_0^2} + \frac{k_{0x}^2}{\omega_0^2 G_0 - \omega_{ce}^2}\right\} E_{rz}^* \tag{3.68}$$

After substituting J_{rz}^{NL} from Eq.(3.67) into Eq.(3.40) and J_{Az}^{NL} from Eq.(3.68) into Eq.(3.66) accordingly we get

$$\left\{\omega_r^2 - \omega_{pe}^2 - c^2k_r^2 - \frac{\omega_{pe}^2 k_{rx}^2\mu_B B_0}{m_e(\omega_r^2 - \omega_{ce}^2)}\tanh\left(\frac{\mu_B B_0}{k_B T_e}\right)\right\} E_{rz}$$

$$= -\frac{\omega_r\omega_{pe}^2 e}{k_{Az}k_B T_e}\phi_0 E_{Az}^*\left\{\frac{k_{0z}}{\omega_0}\left(1 + \frac{k_{0z}}{k_{Az}}\frac{\omega_A}{\omega_0}\right) + \frac{\omega_A}{k_{Az}}\left(1 + \frac{k_{Az}k_{0z}}{\omega_0\omega_A}v_{te}^2\right)\frac{k_{0x}^2}{\omega_0^2 G_0 - \omega_{ce}^2}\right\} \tag{3.69}$$

and

$$\left[\frac{\omega_A^2}{k_{Az}^2\lambda_{De}^2} - \omega_{pi}^2 + c^2k_{Ax}^2 S_p - c^2k_{Ax}^2k_{Az}^2\left(1 - S_p + \frac{v_{ti}^2}{v_A^2}\right)\frac{\left(v_{ti}^2 - v_A^2 S_p\right)}{\left(\omega_A^2 - v_A^2k_{Az}^2(1 - S_p)\right)}\right] E_{Az}$$

$$= \frac{e\omega_A\omega_{pe}^2}{m_e\omega_r}\left\{\frac{k_{0z}^2}{\omega_0^2} + \frac{k_{0x}^2}{\omega_0^2 G_0 - \omega_{ce}^2}\right\}\phi_0 E_{rz}^* \tag{3.70}$$

Taking complex conjugate of Eq.(3.69) and multiplying with Eq.(3.70), we get the coupled expression of three waves, as

$$D_r\epsilon_A = -\mu \tag{3.71}$$

where

$$D_r = \left\{\omega_r^2 - \omega_{pe}^2 - c^2k_r^2 - \frac{\omega_{pe}^2 k_{rx}^2\mu_B B_0}{m_e(\omega_r^2 - \omega_{ce}^2)}\tanh\left(\frac{\mu_B B_0}{k_B T_e}\right)\right\},$$

$$\epsilon_A = \left[\frac{\omega_A^2}{k_{Az}^2\lambda_{De}^2} - \omega_{pi}^2 + c^2k_{Ax}^2 S_p - c^2k_{Ax}^2k_{Az}^2\left(1 - S_p + \frac{v_{ti}^2}{v_A^2}\right)\frac{\left(v_{ti}^2 - v_A^2 S_p\right)}{\left(\omega_A^2 - v_A^2k_{Az}^2(1 - S_p)\right)}\right]$$

and

$$\mu = \frac{\omega_{pe}^4 e^2\omega_A}{k_{Az}k_B T_e m_e}|\phi_0|^2\left\{\frac{k_{0z}}{\omega_0}\left(1 + \frac{k_{0z}}{k_{Az}}\frac{\omega_A}{\omega_0}\right) + \frac{\omega_A}{k_{Az}}\left(1 + \frac{k_{Az}k_{0z}}{\omega_0\omega_A}v_{te}^2\right)\frac{k_{0x}^2}{\omega_0^2 G_0 - \omega_{ce}^2}\right\}\left\{\frac{k_{0z}^2}{\omega_0^2} + \frac{k_{0x}^2}{\omega_0^2 G_0 - \omega_{ce}^2}\right\}$$

Eq.(3.71) is the nonlinear dispersion relation of the three wave interaction. In Eq.(3.71) μ is the coupling parameter of the given three wave interaction problem. D_r and ϵ_A are coupled through μ which comes from pump. If the field of pump wave goes to zero i.e., $\phi_0 \rightarrow 0$, then the three modes will be decoupled. Spin modified linear dispersion relation of O-mode and shear Alfvén wave can be found out by setting $D_r = 0$ and $\epsilon_A = 0$.

3.4 Growth Rate

In order to obtain the growth of this three-wave parametric instability, we expand $\epsilon_A(\omega_A, k_A)$ and $D_r(\omega_r, k_r)$ around the resonant frequencies [12]–[14], [36]–[38],

$$\begin{aligned} \omega_r &= \omega_r + i\gamma, \qquad (3.72) \\ \omega_A &= \omega_A + i\gamma, \\ \epsilon_A(\omega_A, \mathbf{k}_A) &= \epsilon_A^R(\omega_A, \mathbf{k}_A) + i\gamma \frac{\partial \epsilon_A^R}{\partial \omega_A}, \qquad (3.73) \\ |D_r|(\omega_r, \mathbf{k}_r) &= |D_r^R|(\omega_r, \mathbf{k}_r) + i\gamma \frac{\partial |D_r^R|}{\partial \omega_r}, \end{aligned}$$

where $\gamma \ll \omega_A$. At resonance $\epsilon_A^R = 0$ and $|D_r^R| = 0$, so Eq.(3.72) yields

$$(\gamma + \gamma_{Dr})(\gamma + \gamma_{DA}) \equiv \frac{-\mu}{\frac{\partial \epsilon_A^R}{\partial \omega_A}\frac{\partial |D_r^R|}{\partial \omega_r}} \equiv \gamma^2, \qquad (3.74)$$

$$\frac{\partial |D_r^R|}{\partial \omega_r} = 2\omega_r \left\{ 1 + \frac{\omega_{pe}^2 \mu_B B_0 k_{rx}^2}{m_e(\omega_r^2 - \omega_{ce}^2)^2} \tanh\left(\frac{\mu_B B_0}{k_B T_e}\right) \right\} \qquad (3.75)$$

$$\frac{\partial \epsilon_A^R}{\partial \omega_A} = 2\omega_A \left[\frac{1}{k_{Az}^2 \lambda_{De}^2} + c^2 k_{Ax}^2 k_{Az}^2 \left(1 - S_p + \frac{v_{ti}^2}{v_A^2}\right) \frac{\left(v_{ti}^2 - v_A^2 S_p\right)}{\left(\omega_A^2 - v_A^2 k_{Az}^2 (1 - S_p)\right)^2} \right] \qquad (3.76)$$

Now we make numerical calculations of γ/ω_A as a function of various parameters of interest in a magneto-plasma.

3.5 Numerical Results and Graphical Description

The numerical appreciation of the results of our theory is achieved from the calculations of the growth rates of three wave instability for the following set of typical parameters of the fusion plasmas in cgs system [55, 72], $n_{0e} = 1 \times 10^{21} cm^{-3}$; $n_{0i} = 1 \times 10^{21} cm^{-3}$; $B_0 = 5 \times 10^6 G$; $T_e = 10^5 K$; $T_i = 10^3 K$; $\phi_0 = 1 statvolt$; $m_i = 1.6726 \times 10^{-24} g$; $\theta_1 = 1 - 3.5^0$. The wave parameters and the growth rates for the fixed angles $\theta_1 = 3^0$, $\theta_2 = 0.57^0$ are measured as $k_0 = 1 \times 10^4 cm^{-1}$; $k_r = 1.0005 \times 10^4 cm^{-1}$; $k_A = 1 \times 10^2 cm^{-1}$; $\omega_0 = 1.7862 \times 10^{15} rad/\sec$; $\omega_A = 3.4441 \times 10^9 rad/\sec$; $\omega_r \simeq 1.7862 \times 10^{15} rad/\sec$; $\gamma = 7.8067 \times 10^7 rad/\sec(without\ spin)$ and $\gamma = 7.3782 \times 10^7 rad/\sec(with\ spin)$. Here θ_1 is the angle made by SAW with z-axes and θ_2 is the angle which makes the UH wave with x-axes.[1]

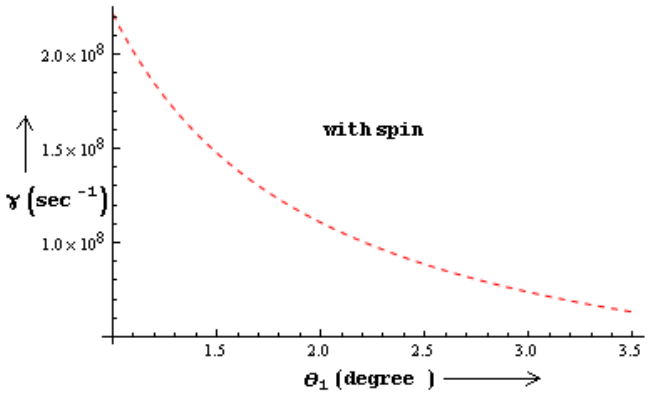

Figure 3-2: Relationship of the growth rate γ vs. θ_1 (with spin effect).

[1] In this chapter growth rate is plotted on new data which is more suitable than published in our Ref.[65].

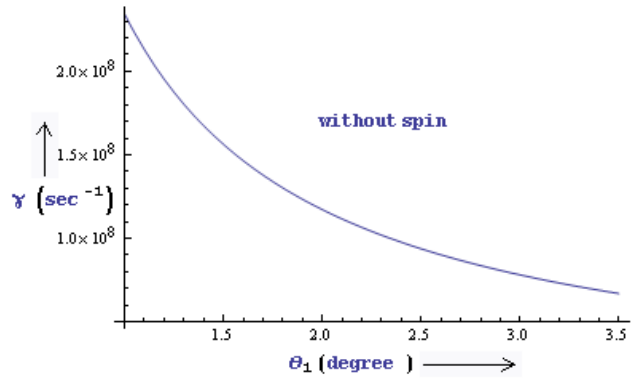

Figure 3-3: Relationship of the growth rate γ vs. θ_1 (without spin effect).

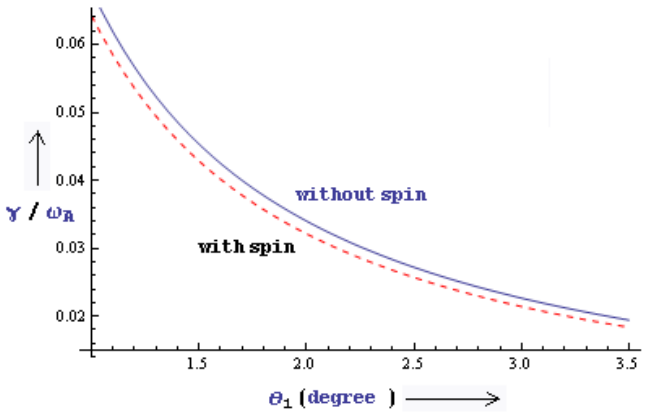

Figure 3-4: Relationship of the normalized growth rate γ/ω_A vs θ_1.

Fig.3-2 elaborates the variation of the growth rate γ of parametric instability including the spin effect of electrons as a function of angle 'θ_1'. In order to get the numerical results of the growth rate without spin effect we simply substitute $\mu_B \to 0$ in Eqs.(3.75 and 3.76). In Fig.3-3 the growth rate γ of parametric instability without spin effect of electrons is plotted as a function of angle 'θ_1'.

Figs.(3-2 and 3-3) elaborate that on increasing angle between the direction of propagation of the low frequency electromagnetic mode (shear Alfvén wave) and the static magnetic field B_0, the growth rate decreases gradually. Fig.3-4 shows the variation of the normalized growth rate γ/ω_A as a function of θ_1 for spin and without spin effect.

3.6 Discussion

In this chapter, we have investigated the parametric decay instability of Upper Hybrid Wave in xz-plane into a low-frequency electromagnetic shear Alfvén wave propagating nearly parallel to the direction of static magnetic field and another electromagnetic sideband, viz. O-mode propagating along the perpendicular direction of magnetic field in a thermal homogeneous classical magneto-plasma. The hydrodynamic model with quantum effect arising through electron spin dynamics in static magnetic field has been employed to obtain linear and nonlinear response of electrons and ions. Here, electrons with spin-up and spin-down are regarded as different fluids.

The growth rate of three wave parametric instability decreases with the inclusion of the spin properties of the electrons. This leads to the stability of the plasma environment. Spin plays the paramagnetic behavior which is important for the confinement of the plasmas. A numerical calculation of the growth rate of three wave parametric instability has been made with typical parameters of fusion plasmas. At fixed scattering angles $\theta_1 = 3^0$, $\theta_2 = 0.57^0$ the growth rate $\gamma = 7.3782 \times 10^7 rad/\sec$ is achieved for spin electron dynamics and $\gamma = 7.8067 \times 10^7 rad/\sec$ without the spin. The expression $S_p = \frac{4\pi n_{0e}\mu_B}{B_0} tanh\left(\frac{\mu_B B_0}{k_B T_e}\right)$ shows that the effect of spin on growth rate increases on increasing the n_{0e}. The spin magnetization current density(See Eqs.(3.38, 3.62 and 3.63)) is directly proportional to the difference of two population $(n_{0+} - n_{0-})$ which in turn proportional to n_{0e}. Although the spin effect of electron is quantum nature but in this chapter we emphasis that the spin effect can be seen even in classical plasma environments.

The spin contribution of electrons does not change the dispersion relation of electrostatic upper hybrid wave. This only modifies the dispersion relations of electromagnetic waves (Shear Alfveń wave and O-mode). This is because, when an electromagnetic perturbation enters the system, the spin-ponderomotive force separates the two populations, which in turn modifies the magnetic field [55].

The important contribution of this study is to provide further physical insight into the parametric instabilities in uniform magneto-plasmas with a special spin property of electrons. Three wave interaction may be the main mechanism for the generation of electromagnetic waves in aurora, ionosphere and in magnetosphere.

Chapter 4

Spin Effect on Parametric Decay of Oblique Langmuir Wave in Degenerate Magneto-plasmas

The spin -1/2 effect of electrons on the parametric decay instability of oblique Langmuir wave into low-frequency electromagnetic shear Alfven wave and Left-Handed Circularly Polarized wave (LHCP) has been studied in detail, in electron-ion quantum plasma immersed in the uniform external magnetic field. The quantum magneto-hydrodynamic (QMHD) model has been used to investigate the quantum effects due to electron spin, Fermi pressure and effective quantum force. Nonlinear dispersion relations and growth rate of the problem have been derived analytically. It has been shown that the spin of electrons has considerable effect on the growth rate of parametric instability problem for the plasma regime where external magnetic field B_0 is below the quantum critical magnetic field strength $B_Q = 4.4138 \times 10^{13} G$ [68].

4.1 Introduction

In this chapter, we present the nonlinear interaction of three waves in which an oblique Langmuir wave or an electron plasma wave (EPW) decay parametrically into LHCP and low-frequency electromagnetic shear Alfven wave (SAW), in a spin degenerate magneto-plasmas. The EPW with frequency ω_0 and wave vector $\mathbf{k}_0$ as a pump is propagating in xz-plane which makes a

small angle with z-axis. LHCP propagates along the external magnetic field $B_0\hat{z}$ with frequency ω_L and wave vector $\mathbf{k}_L$, and the excited SAW lies in xz-plane at a small angle with z-axis (See Fig. 4-1).

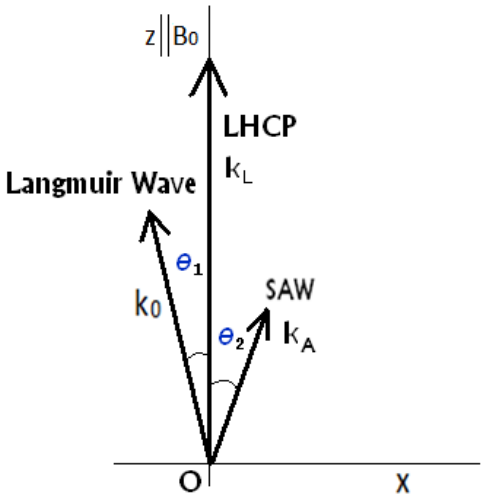

Figure 4-1: Schematic diagram of propagation of EPW, LHCP and SAW in xz-plane.

For parametric interaction, these three waves must satisfy the following phase matching conditions [4],

$$\omega_0 = \omega_L + \omega_A, \tag{4.1}$$

and

$$\mathbf{k}_0 = \mathbf{k}_L - \mathbf{k}_A. \tag{4.2}$$

Eq.(4.1) and Eq.(4.2) explain the law of conservation of energy and momentum in three wave interaction.

Quantum effects are only due to electrons whereas ions are treated as classical and the temperature ordering is $T_i < T_e < T_{Fe}$. Electrons are considered as three-dimensional (3D) Fermi gas and equation of state for such a gas is [28, 73] $P_e = \frac{2}{5}\frac{k_B T_{Fe} n_e^3}{n_{0e}^2}\left[1 + \frac{5}{12}\pi^2\left(\frac{T_e}{T_{Fe}}\right)^2\right]$, where $T_{Fe} = \hbar^2(3\pi^2 n_{0e})^{2/3}/2k_B m_e$ is the electron Fermi temperature and T_e is the electron thermal temperature.

The spin contribution of electrons enters through spin magnetization current. Electrons

with spin up and spin down are supposed different fluids and for the plasma regime where $T_{Fe} > T_e$, the unperturbed density difference of the two spin populations can be [61, 66]

$$n_{0+} - n_{0-} = n_{0e}\frac{3}{2}\frac{\mu_B B_0}{k_B T_{Fe}}. \tag{4.3}$$

This chapter is organized in the following manner. In Section 4.2 we have introduced the governing equations together with some necessary algebra for each wave mode (EPW, LHCP and SAW). In Section 4.3 we have derived the linear and nonlinear response functions and growth rate is calculated in Section 4.4. In Section 4.5, the growth rate of parametric instability for dense astrophysical environments (quantum magneto-plasma) has been plotted. In Section 4.6 we briefly explain why the growth rate decreases with the inclusion of spin of electrons and how the spin of electrons plays an important role in the stability of the plasmas.

4.2 Mathematical Model

The nonlinear interaction of waves in magnetized spin quantum plasma is governed by the following fluid equations, the Maxwell's equations and the spin evolution equation,

$$\partial_t \mathbf{v}_j = \frac{q_j \mathbf{E}}{m_j} + \mathbf{v}_j \times \omega_{cj}\widehat{z} - \frac{\nabla P_j}{m_j n_j} + \frac{2\mu_j}{\hbar m_j} S_j^a \nabla B_a + \frac{\hbar^2}{2m_j^2}\nabla\left(\frac{\nabla^2\sqrt{n_j}}{\sqrt{n_j}}\right), \tag{4.4}$$

$$\partial_t n_j + \nabla.(n_j \mathbf{v}_j) = 0, \tag{4.5}$$

$$\nabla \times \mathbf{E} = -\frac{1}{c}\partial_t \mathbf{B}, \tag{4.6}$$

$$c\nabla \times \mathbf{B} = 4\pi \mathbf{J} + \partial_t \mathbf{E}, \tag{4.7}$$

$$\nabla.\mathbf{E} = 4\pi \sum_j q_j n_j, \tag{4.8}$$

$$\left(\partial_t + \mathbf{v}_j.\nabla\right)\mathbf{S}_j = \frac{2\mu_j}{\hbar}\mathbf{S}_j \times \mathbf{B} \tag{4.9}$$

where $j = i$ (ions), e (electrons), $+$ (spin up electrons), $-$ (spin down electrons), P_j is the statistical pressure which contains both the Fermi pressure and the thermal pressure [28]. Note that apart from usual equations (4.4–4.8), we now have an additional equation - so called spin

evolution equation - for mathematical treatment of additional spin variable S_j. The quantum effects represented by the last term on the right-hand side of Eq.(4.4) are due to the so-called Bohm potential. For simplicity, the quantum effects are taken only for electrons whereas ions are treated as classical.

The current density in Eq.(4.7) can be expressed as

$$\mathbf{J} = \mathbf{J}^L + \mathbf{J}^{NL} \tag{4.10}$$

where $\mathbf{J}^{NL}$ is a nonlinear current density due to the coupling of two waves in plasma. The linear current density $\mathbf{J}^L$ for spin plasmas is due to charge current density J_q and magnetization current density J_m

$$\mathbf{J^L} = \mathbf{J}_q + \mathbf{J}_m, \qquad \mathbf{J}_q = \sum_j q_j n_j \mathbf{v}_j \tag{4.11}$$

and

$$\mathbf{J}_m = \sum_j \nabla \times \mathbf{M}_j = \sum_j \nabla \times \frac{2\mu_j n_j}{\hbar} \mathbf{S}_j \tag{4.12}$$

For three wave interaction problem we can decompose all the physical quantities in the following manner:

$$n_j = n_{0j} + n_{1j}^0 + n_{1j}^A, \qquad \mathbf{v}_j = \mathbf{v}_j^0 + \mathbf{v}_j^L + \mathbf{v}_j^A, \tag{4.13}$$

$$\mathbf{E} = \mathbf{E}_0 + \mathbf{E}_L + \mathbf{E}_A \tag{4.14}$$

where the superscripts 0, L and A in Eq.(3.13) and subscripts 0, L and A in Eq.(3.14) represent the corresponding perturbed quantities associated with the pump wave, L-wave and SAW respectively. The density perturbation n_{1j}^L is zero in the field of L-wave. All the perturbed physical quantities behave sinusoidally.

4.2.1 Oblique Langmuir Wave

Consider the propagation of a finite amplitude electrostatic EPW in a homogeneous magnetoplasma. The static ambient magnetic field $\mathbf{B}_0$ is along the z-axis. The electric field of the

high-frequency wave can be written as

$$\mathbf{E}_0 = (\widehat{x}E_{0x} + \widehat{z}E_{0z}) \exp(-i\omega_0 t + i\mathbf{k}_0.\mathbf{r}_0) + c.c, \tag{4.15}$$

where $c.c$ stands for the complex conjugate and $E_{0x} < E_{0z}$. The frequency ω_0 and the wave vector $\mathbf{k}_0$ are related by the linear dispersion relation

$$\omega_0^2 = \omega_H^2 + k_0^2 V_{Fe}'^2 - \frac{k_{0z}^2}{k_0^2} \frac{\left(\omega_{pe}^2 + k_0^2 V_{Fe}^2\right) \omega_{ce}^2}{\omega_H^2 + k_0^2 V_{Fe}^2}, \tag{4.16}$$

where $\omega_H^2 = \omega_{pe}^2 + \omega_{ce}^2$, $V_{F0}^2 = V_{Fe}^2 + k_0^2\hbar^2/4m_e^2$, $V_{Fe}^2 = \frac{6}{5}\frac{k_B T_{Fe}}{m_e}\left[1 + \frac{5}{12}\pi^2\left(\frac{T_e}{T_{Fe}}\right)^2\right]$.

The components of electron velocity in the field of pump EPW can be determined from equations (4.4 and 4.5) as

$$v_{xe}^0 = -\frac{ie\omega_0 E_{0x}}{m_e\left(\omega_0^2 G_0 - \omega_{ce}^2\right)} - \frac{k_{0x}k_{0z}V_{F0}^2}{\left(\omega_0^2 G_0 - \omega_{ce}^2\right)} \frac{ieE_{0z}}{\omega_0 m_e F_0}\ , \tag{4.17}$$

$$v_{ye}^0 = \frac{e\omega_{ce}E_{0x}}{m_e\left(\omega_0^2 G_0 - \omega_{ce}^2\right)} + \frac{k_{0x}k_{0z}V_{F0}^2}{\left(\omega_0^2 G_0 - \omega_{ce}^2\right)} \frac{e\omega_{ce}E_{0z}}{\omega_0^2 m_e F_0} \tag{4.18}$$

and

$$v_{ze}^0 = -\frac{k_{0z}k_{0x}V_{F0}^2}{\omega_0 F_0} \frac{ieE_{0x}}{m_e\left(\omega_0^2 G_0 - \omega_{ce}^2\right)} - \frac{ieE_{0z}}{\omega_0 m_e F_0}\left(1 + \frac{k_{0x}^2 k_{0z}^2 V_{F0}^4}{\left(\omega_0^2 G_0 - \omega_{ce}^2\right)\omega_0^2 F_0}\right) \tag{4.19}$$

where

$$F_0 = 1 - \frac{k_{0z}^2 V_{F0}^2}{\omega_0^2}, \tag{4.20}$$

and

$$G_0 = \frac{\omega_0^2 - k_0^2 V_{F0}^2}{\omega_0^2 - k_{0z}^2 V_{F0}^2}. \tag{4.21}$$

For electrostatic pump we use $E_{0x} = -ik_{0x}\phi_0$ and $E_{0z} = -ik_{0z}\phi_0$, (ϕ_0 is the potential) and high frequency condition $\omega_0^2 > k_{0x}^2 v_{te}^2$, then above Eqs. (4.17–4.19) reduce to

$$v_{xe}^0 = -\frac{e\omega_0 k_{0x}\phi_0}{m_e\left(\omega_0^2 - \omega_{ce}^2\right)F_0}, \tag{4.22}$$

$$v_{ye}^0 = -\frac{ie\omega_{ce}k_{0x}\phi_0}{m_e\left(\omega_0^2-\omega_{ce}^2\right)F_0} \tag{4.23}$$

and

$$v_{ze}^0 = -\left(1+\frac{k_{0x}^2V_{F0}^2}{(\omega_0^2-\omega_{ce}^2)F_0}\right)\frac{ek_{0z}\phi_0}{\omega_0 m_e F_0} \tag{4.24}$$

From the equation of continuity, the first perturbation in electron number density n_{1e}^0, due to the pump EPW, is obtained as

$$n_{1e}^0 = \frac{n_{0e}}{\omega_0}\left(k_{0x}v_{xe}^0 + k_{0z}v_{ze}^0\right) \tag{4.25}$$

Using values of v_{xe}^0 and v_{ze}^0 from Eq.(4.22) and Eq.(4.24) into the above equation we obtain

$$\frac{n_{1e}^0}{n_{0e}} = -\left(\frac{k_{0z}^2}{\omega_0^2}+\frac{k_{0x}^2}{\left(\omega_0^2-\omega_{ce}^2\right)F_0}\right)\frac{e\phi_0}{m_eF_0}, \tag{4.26}$$

There is no spin contribution in electrostatic pump wave. Spin of electrons only modifies the electromagnetic modes via spin magnetization current density. This pump derives a side band LHCP radiation at $(\omega_L, \mathbf{k}_L)$, which propagates exactly parallel to the external magnetic field. After a while LHCP beats with the pump wave, generates a low frequency force which amplifies the Shear Alfven wave at $(\omega_A, \mathbf{k}_A)$. The excited Shear Alfven wave interacts with the pump wave hence generating a nonlinear current which becomes the source of the modified (or amplified) scattered sideband LHCP radiation. These three waves satisfy the phase matching conditions Eqs.(4.1 and 4.2). In the following sections we will discuss the LHCP wave and SAW.

4.2.2 LHCP Wave

On linearizing the Maxwell equations (4.6 and 4.7) we get the wave equation of the electromagnetic LHCP wave propagating along $\mathbf{B}_0 \| \widehat{z}$,

$$\left(\omega_L^2 - c^2k_L^2\right)\mathbf{E}_L - i4\pi e\omega_L n_{0e}\mathbf{v}_e^L + i4\pi\omega_L\mathbf{J}_m = -i4\pi\omega_L\mathbf{J}_L^{NL}, \tag{4.27}$$

where

$$\mathbf{J}_L^{NL} = -e\left(n_{1e}^{A*}\mathbf{v}_e^0 + n_{1e}^0\mathbf{v}_e^{A*}\right) \tag{4.28}$$

is the nonlinear current density due to coupling of EPW and low frequency SAW, which becomes the source to enhance the LHCP radiation. Here, n_{1e}^{A} and $\mathbf{v}_{e}^{A}$ are perturbed electron number density and velocity in the field of SAW. The asterisk denotes the complex conjugate. The linear electron velocities in the radiation field $\mathbf{E}_L = \widehat{x}E_{Lx} + \widehat{y}E_{Ly}$ can be given from Eq.(4.4)

$$v_{xe}^{L} = \frac{-ie\omega_L}{m_e\left(\omega_L^2 - \omega_{ce}^2\right)}E_{Lx} - \frac{e\omega_{ce}}{m_e\left(\omega_L^2 - \omega_{ce}^2\right)}E_{Ly} \tag{4.29}$$

and

$$v_{ye}^{L} = \frac{-ie\omega_L}{m_e\left(\omega_L^2 - \omega_{ce}^2\right)}E_{Ly} + \frac{e\omega_{ce}}{m_e\left(\omega_L^2 - \omega_{ce}^2\right)}E_{Lx} \tag{4.30}$$

The x- and y-components of magnetization current density $\mathbf{J}_m$ can be written as

$$J_{mx} = -ik_{Lz} \times (M_{+y} + M_{-y}) \tag{4.31}$$

and

$$J_{my} = ik_{Lz} \times (M_{+x} + M_{-x}) \tag{4.32}$$

where

$$M_{+x} = -\frac{2\mu_B c n_{0+} S_{+1}^{x}}{\hbar}, \tag{4.33}$$

$$M_{-x} = -\frac{2\mu_B c n_{0-} S_{-1}^{x}}{\hbar}, \tag{4.34}$$

$$M_{+y} = -\frac{2\mu_B c n_{0+} S_{+1}^{y}}{\hbar} \tag{4.35}$$

and

$$M_{-y} = -\frac{2\mu_B c n_{0-} S_{-1}^{y}}{\hbar} \tag{4.36}$$

are the x- and y-components of the up and down spin magnetizations. The $\mathbf{S}_{1j}$ can be calculated from Eqs.(4.6 and 4.9), that is,

$$\mathbf{S}_{1j} = -\frac{2i\mu_B}{\hbar\omega}\mathbf{S}_{1j} \times \mathbf{B}_0 - \frac{2i\mu_B c}{\hbar\omega^2}(\mathbf{S_0}.\mathbf{E})\mathbf{k} + \frac{2i\mu_B c}{\hbar\omega^2}(\mathbf{k}.\mathbf{S_0})\mathbf{E}, \tag{4.37}$$

The x- and y-components of perturbed spin vector for spin up and spin down electrons in the field of LHCP are

$$S^x_{1+} = \frac{4\mu_B^2 c^2 B_0}{\hbar^2 \omega_L \left(\omega_L^2 - \omega_{cg}^2\right)} k_{rz} S^z_{0+} E_{Ly} + \frac{2i\mu_B c}{\hbar \left(\omega_L^2 - \omega_{cg}^2\right)} k_{Lz} S^z_{0+} E_{Lx}, \tag{4.38}$$

$$S^x_{1-} = \frac{4\mu_B^2 c^2 B_0}{\hbar^2 \omega_L \left(\omega_L^2 - \omega_{cg}^2\right)} k_{rz} S^z_{0-} E_{Ly} + \frac{2i\mu_B c}{\hbar \left(\omega_L^2 - \omega_{cg}^2\right)} k_{Lz} S^z_{0-} E_{Lx}, \tag{4.39}$$

$$S^y_{1+} = -\frac{4\mu_B^2 c^2 B_0}{\hbar^2 \omega_L \left(\omega_L^2 - \omega_{cg}^2\right)} k_{Lz} S^z_{0+} E_{Lx} + \frac{2i\mu_B c}{\hbar \left(\omega_L^2 - \omega_{cg}^2\right)} k_{Lz} S^z_{0+} E_{Ly} \tag{4.40}$$

and

$$S^y_{1-} = -\frac{4\mu_B^2 c^2 B_0}{\hbar^2 \omega_L \left(\omega_L^2 - \omega_{cg}^2\right)} k_{Lz} S^z_{0-} E_{Lx} + \frac{2i\mu_B c}{\hbar \left(\omega_L^2 - \omega_{cg}^2\right)} k_{Lz} S^z_{0-} E_{Ly} \tag{4.41}$$

here, $S^x_{+0} = S^y_{+0} = S^x_{-0} = S^y_{-0} = 0$, $S^z_{+0} = -\frac{\hbar}{2}$, $S^z_{-0} = +\frac{\hbar}{2}$, since, the ambient magnetic field is along z-direction. Using values of S^y_{1+} and S^y_{1-} from Eq.(4.40) and Eq.(4.41) into Eq.(4.35) and Eq.(4.36) respectively we get

$$M_{+y} = -\frac{2\mu_B^2 c^2 k_{Lz}}{\hbar \left(\omega_L^2 - \omega_{cg}^2\right)} \left(\frac{2\mu_B c B_0}{\hbar \omega_L} E_{Lx} - iE_{Ly}\right) n_{0+} \tag{4.42}$$

and

$$M_{-y} = \frac{2\mu_B^2 c^2 k_{Lz}}{\hbar \left(\omega_L^2 - \omega_{cg}^2\right)} \left(\frac{2\mu_B c B_0}{\hbar \omega_L} E_{Lx} - iE_{Ly}\right) n_{0-} \tag{4.43}$$

Substituting these values of M_{+y} and M_{-y} into Eq.(4.31) we get the x-component of the magnetization current density in the field of LHCP

$$J_{mx} = \left(\frac{i\omega_{ce}}{\omega_L} E_{Lx} + E_{Ly}\right) \frac{\omega_{cg} c^2 k_{Lz}^2 Sp}{4\pi \left(\omega_L^2 - \omega_{cg}^2\right)} \tag{4.44}$$

where $Sp = \frac{6\pi n_{0e} \mu_B^2}{k_B T_{Fe}}$. Here, $\omega_{cg}^2 = \frac{4\mu_B^2 B_0^2}{\hbar^2} \approx \omega_{ce}^2$, is the characteristic spin precession frequency. We have used the unperturbed density difference $n_{0+} - n_{0-} = n_{0e} \frac{3}{2} \frac{\mu_B B_0}{k_B T_{Fe}}$ of the two spin populations for plasma regime where $T_{Fe} > T_e$ [61, 66].

Now putting values of S^x_{1+} and S^x_{1-} from Eq.(4.38) and Eq.(4.39) into Eq.(4.33) and Eq.(4.34) respectively we get

$$M_{+x} = \frac{2\mu_B^2 c^2 k_{Lz}}{\hbar \left(\omega_L^2 - \omega_{cg}^2\right)} \left(\frac{2\mu_B c B_0}{\hbar \omega_L} E_{Ly} + iE_{Lx}\right) n_{0+} \tag{4.45}$$

and

$$M_{-x} = -\frac{2\mu_B^2 c^2 k_{Lz}}{\hbar\left(\omega_L^2 - \omega_{cg}^2\right)}\left(\frac{2\mu_B c B_0}{\hbar\omega_L}E_{Ly} + iE_{Lx}\right)n_{0-} \tag{4.46}$$

Substituting these values of M_{+x} and M_{-x} into Eq.(4.32) we get the y-component of the magnetization current density in the field of LHCP

$$J_{my} = \left(i\frac{\omega_{ce}}{\omega_L}E_{Ly} - E_{Lx}\right)\frac{\omega_{cg}c^2k_{Lz}^2 Sp}{4\pi\left(\omega_L^2 - \omega_{cg}^2\right)} \tag{4.47}$$

Now by using the Eqs.(4.29, 4.30, 4.44 and 4.47), we can get the x- and y-components of Eq.(4.27) as

$$\left(\omega_L^2 - c^2k_{Lz}^2 - \alpha\right)E_{Lx} + i\beta E_{Ly} = -i4\pi\omega_L J_{Lx}^{NL} \tag{4.48}$$

and

$$-i\beta E_{Lx} + \left(\omega_L^2 - c^2k_L^2 - \alpha\right)E_{Ly} = -i4\pi\omega_L J_{Ly}^{NL} \tag{4.49}$$

where

$$\alpha = \frac{\left(\omega_{pe}^2\omega_L^2 + \omega_{ce}^2c^2k_{Lz}^2Sp\right)}{\left(\omega_L^2 - \omega_{ce}^2\right)}, \tag{4.50}$$

$$\beta = \frac{\omega_L\omega_{ce}\left(\omega_{pe}^2 + c^2k_{Lz}^2Sp\right)}{\left(\omega_L^2 - \omega_{ce}^2\right)}, \tag{4.51}$$

$$J_{Lx}^{NL} = -e\left(n_{1e}^{A*}v_{xe}^0 + n_{1e}^0v_{xe}^{A*}\right) \tag{4.52}$$

and

$$J_{Ly}^{NL} = -e\left(n_{1e}^{A*}v_{ye}^0 + n_{1e}^0v_{ye}^{A*}\right) \tag{4.53}$$

4.2.3 Shear Alfven Wave

Kinetic Alfven waves [47]–[49] arise in a low-β ($m_e/m_i < \beta = 8\pi n_{0e}k_BT_{eff}/B_0^2 < 1$) plasma with $k_{Az}v_{ti} < \omega_A << \omega_{ci}$, $k_{Az}V_{Fe}$, propagating in xz-plane and making a small angle with $\mathbf{B}_0\|\widehat{z}$. Here $T_{eff} = \frac{6}{5}T_{Fe}\left[1 + \frac{5}{12}\pi^2\left(\frac{T_e}{T_{Fe}}\right)^2\right] = \frac{m_eV_{Fe}^2}{k_B}$ and v_{ti} is the ion thermal velocity. The response of the plasma particles due to SAW in this three-wave parametric process, in the presence of the ambient magnetic field $\mathbf{B}_0$, is governed by the Eqs.(4.6 and 4.7) with script A for shear Alfven wave. The wave equation is

$$\begin{aligned}\left(\omega_A^2 - c^2k_A^2\right)\mathbf{E}_A + c^2\left(\mathbf{k}_A.\mathbf{E}_A\right)\mathbf{k}_A + i4\pi\omega_A\left(\sum_j q_j n_{0j}\mathbf{v}_j^A + \mathbf{J}_m\right) \\ = -i4\pi\omega_A\mathbf{J}_A^{NL},\end{aligned} \tag{4.54}$$

where

$$\mathbf{J}_A^{NL} = -e\left(n_{1e}^{L*}\mathbf{v}_e^0 + n_{1e}^0\mathbf{v}_e^{L*}\right), \tag{4.55}$$

is the nonlinear current density, being generated by the beating of the pump wave and LHCP radiation. The x- and z-components of the Eq.(4.54) are

$$\begin{aligned}\left(\omega_A^2 - c^2k_{Az}^2\right)E_{Ax} + c^2k_{Ax}k_{Az}E_{Az} - i4\pi\omega_A e n_{0e}v_{xe}^A + i4\pi\omega_A e n_{0i}v_{xi}^A + i4\pi\omega_A J_{mx} \\ = -i4\pi\omega_A J_{Ax}^{NL}\end{aligned} \tag{4.56}$$

and

$$\begin{aligned}\left(\omega_A^2 - c^2k_{Ax}^2\right)E_{Az} + c^2k_{Ax}k_{Az}E_{Ax} - i4\pi\omega_A e n_{0e}v_{ze}^A + i4\pi\omega_A e n_{0i}v_{zi}^A + i4\pi\omega_A J_{mz} \\ = -i4\pi\omega_A J_{Az}^{NL}\end{aligned} \tag{4.57}$$

where

$$J_{Ax}^{NL} = -en_{1e}^0 v_{xe}^{L*} \tag{4.58}$$

and

$$J_{Az}^{NL} = 0 \tag{4.59}$$

Here we have taken $v_{ze}^L = 0$ and $n_{1e}^L = 0$ due to electromagnetic LHCP radiations. For low frequency electromagnetic Shear Alfven wave, the electrons are inertia less, $k_{Az} >> k_{Ax}$ and $E_{Ax} >> E_{Az}$. Under these conditions, the perturbed electron number density and the velocity components of species for SAW can be found out from Eqs.(4.4 and 4.5) as:

$$\frac{n_{1e}^A}{n_{0e}} = \frac{ieE_{Az}}{m_e k_{Az}V_{FA}^2}, \tag{4.60}$$

$$v_{xe}^A = 0, \tag{4.61}$$

$$v_{ye}^A = \frac{e}{m_e\omega_{ce}}E_{Ax} \to 0, \tag{4.62}$$

$$v_{ze}^{A} = \frac{ie\omega_A E_{Az}}{m_e k_{Az}^2 V_{FA}^2}, \tag{4.63}$$

$$v_{xi}^{A} = \frac{-ie\omega_A E_{Ax}}{\omega_{ci}^2 m_i} - \frac{k_{Ax} v_{ti}^2}{\omega_{ci}^2} \frac{iek_{Az} E_{Az}}{\omega_A m_i}, \tag{4.64}$$

and

$$v_{zi}^{A} = -\frac{iek_{Ax} k_{Az} v_{ti}^2 E_{Ax}}{\omega_{ci}^2 \omega_A m_i} + \frac{ieE_{Az}}{\omega_A m_i}. \tag{4.65}$$

The spin of electrons will contribute through the magnetization current density $\mathbf{J}_m$, so the x- and z-components of $\mathbf{J}_m$ in the field of SAW can be written as

$$J_{mx} = -ik_{Az} \times (M_{+y} + M_{-y}) \tag{4.66}$$

and

$$J_{mz} = ik_{Ax} \times (M_{+y} + M_{-y}) \tag{4.67}$$

here

$$M_{+y} = -\frac{2\mu_B c n_{0+} S_{+1}^{y}}{\hbar} \tag{4.68}$$

and

$$M_{-y} = -\frac{2\mu_B c n_{0-} S_{-1}^{y}}{\hbar} \tag{4.69}$$

The y-component of perturbed spin vector for spin up and spin down electrons in the field of LHCP are given from Eq.(4.37) as

$$S_{+1}^{y} = \frac{c\hbar k_{Ax}}{2\omega_A B_0} E_{Az} - \frac{c\hbar k_{Az}}{2\omega_A B_0} E_{Ax} \tag{4.70}$$

and

$$S_{-1}^{y} = -\frac{c\hbar k_{Ax}}{2\omega_A B_0} E_{Az} + \frac{c\hbar k_{Az}}{2\omega_A B_0} E_{Ax} \tag{4.71}$$

Here, we have used $S_{+0}^{z} = -\frac{\hbar}{2}$, $S_{-0}^{z} = \frac{\hbar}{2}$ and $n_{0+} - n_{0-} = n_{0e}\frac{3}{2}\frac{\mu_B B_0}{k_B T_{Fe}}$. Now putting values of S_{+1}^{y} from Eq.(4.70) and S_{-1}^{y} from Eq.(4.71) into Eq.(4.68) and Eq.(4.69) respectively we get

$$M_{+y} = -\frac{\mu_B c^2 n_{0+}}{\omega_A B_0} (k_{Ax} E_{Az} - k_{Az} E_{Ax}) \tag{4.72}$$

and

$$M_{-y} = \frac{\mu_B c^2 n_{0+}}{\omega_A B_0} \left(k_{Ax} E_{Az} - k_{Az} E_{Ax}\right) \tag{4.73}$$

Using these values of M_{+y} from Eq.(4.72) and M_{-y} from Eq.(4.73) into Eq.(4.66) and Eq.(4.67) we get

$$J_{mx} = i k_{Az} \frac{c^2 Sp}{4\pi\omega_A} \left(k_{Ax} E_{Az} - k_{Az} E_{Ax}\right), \tag{4.74}$$

and

$$J_{mz} = -i k_{Ax} \frac{c^2 Sp}{4\pi\omega_A} \left(k_{Ax} E_{Az} - k_{Az} E_{Ax}\right). \tag{4.75}$$

Substituting the Eqs.(4.58, 4.61, 4.64 and 4.74) into Eq.(4.56) we get

$$\left[\omega_A^2 \left(1 + \frac{\omega_{pi}^2}{\omega_{ci}^2}\right) - c^2 k_{Az}^2 \left(1 - Sp\right)\right] E_{Ax} + \left(\frac{\omega_{pi}^2}{\omega_{ci}^2} v_{ti}^2 - c^2 Sp\right) k_{Ax} k_{Az} E_{Az} = i4\pi e \omega_A n_{1e}^0 v_{xe}^{L*}, \tag{4.76}$$

and substituting the Eqs.(4.59, 4.63, 4.65 and 4.75) into Eq.(4.57) we get

$$\left(\frac{\omega_{pi}^2}{\omega_{ci}^2} v_{ti}^2 + c^2 \left(1 - Sp\right)\right) k_{Ax} k_{Az} E_{Ax} + \left(\frac{\omega_A^2}{k_{Az}^2 \lambda_{FA}^2} - \omega_{pi}^2 + c^2 k_{Ax}^2 Sp\right) E_{Az} = 0, \tag{4.77}$$

where $\lambda_{FA}^2 = \frac{V_{FA}^2}{\omega_{pe}^2}$, $V_{FA}^2 = V_{Fe}^2 + k_A^2 \hbar^2 / 4m_e^2$ and $k_{Az}^2 \lambda_{FA}^2 << 1$. Eliminating E_{Ax} from Eqs.(4.76 and 4.77) we get

$$\epsilon_A E_{Az} = i4\pi e \omega_A n_{1e}^0 v_{xe}^{L*} \tag{4.78}$$

Here

$$\epsilon_A = c^2 k_{Ax} k_{Az} \left(\frac{v_{ti}^2}{v_A^2} - Sp\right) - \left(\frac{\omega_A^2}{k_{Az}^2 \lambda_{FA}^2} - \omega_{pi}^2 + c^2 k_{Ax}^2 Sp\right) \frac{\left(\omega_A^2 \left(1 + \frac{c^2}{v_A^2}\right) - c^2 k_{Az}^2 \left(1 - Sp\right)\right)}{c^2 k_{Ax} k_{Az} \left(1 - Sp + \frac{v_{ti}^2}{v_A^2}\right)} \tag{4.79}$$

By taking $\epsilon_A = 0$, we can get the spin modified linear dispersion relation of the SAW. On the other hand, the right hand side of the Eq.(4.78) is the coupling of the pump wave and the LHCP which provides the source to enhance the SAW.

4.3 Nonlinear Dispersion Relations

Using values of v_{xe}^0, v_{ye}^0, n_{1e}^0, v_{xe}^A, v_{ye}^A and n_{1e}^A, from Eqs.(4.22, 4.23, 4.26, 4.61, 4.62 and 4.60), into Eqs.(4.52 and 4.53) respectively, we get

$$J_{Lx}^{NL} = -\frac{ie}{m_e} \frac{\omega_0 k_{0x}}{4\pi k_{Az} \lambda_{FA}^2 F_0 \left(\omega_0^2 - \omega_{ce}^2\right)} E_{Az}^* \phi_0 \tag{4.80}$$

and

$$J_{Ly}^{NL} = \frac{e}{m_e} \frac{\omega_{ce} k_{0x}}{4\pi k_{Az} \lambda_{FA}^2 F_0 \left(\omega_0^2 - \omega_{ce}^2\right)} E_{Az}^* \phi_0 \tag{4.81}$$

By using these values of J_{Lx}^{NL} from Eq.(4.80) and J_{Ly}^{NL} from Eq.(4.81) into Eq.(4.48) and Eq.(4.49) respectively we get

$$\left(\omega_L^2 - c^2 k_{Lz}^2 - \alpha\right) E_{Lx} + i\beta E_{Ly} = -\frac{e}{m_e} \frac{\omega_L \omega_0 k_{0x}}{k_{Az} \lambda_{FA}^2 F_0 \left(\omega_0^2 - \omega_{ce}^2\right)} E_{Az}^* \phi_0 \tag{4.82}$$

and

$$-i\beta E_{Lx} + \left(\omega_L^2 - c^2 k_L^2 - \alpha\right) E_{Ly} = -\frac{ie}{m_e} \frac{\omega_L \omega_{ce} k_{0x}}{k_{Az} \lambda_{FA}^2 F_0 \left(\omega_0^2 - \omega_{ce}^2\right)} E_{Az}^* \phi_0 \tag{4.83}$$

Now substituting values of n_{1e}^0 from Eq.(4.26) and v_{xe}^L from Eq.(4.29) into Eq.(4.78), we obtain

$$\epsilon_A E_{Az} = \left(\omega_r E_{Lx}^* + i\omega_{ce} E_{Ly}^*\right) H \phi_0 \tag{4.84}$$

where

$$H = \frac{\omega_A \omega_{pe}^2}{\left(\omega_L^2 - \omega_{ce}^2\right)} \left(\frac{k_{0z}^2}{\omega_0^2} + \frac{k_{0x}^2}{\left(\omega_0^2 - \omega_{ce}^2\right) F_0} \right) \frac{e}{m_e F_0} \tag{4.85}$$

Now taking complex conjugate of Eq.(4.84) and multiplying with Eq.(4.82), we get

$$\begin{aligned} &\left\{ \left(\omega_L^2 - c^2 k_{Lz}^2 - \alpha\right) E_{Lx} + i\beta E_{Ly} \right\} \epsilon_A \\ &= -\left(\omega_L E_{Lx} - i\omega_{ce} E_{Ly}\right) \frac{e}{m_e} \frac{\omega_L \omega_0 k_{0x}}{k_{Az} \lambda_{FA}^2 F_0 \left(\omega_0^2 - \omega_{ce}^2\right)} H \left|\phi_0\right|^2 \end{aligned} \tag{4.86}$$

Here, $\left|\phi_0\right|^2 = \phi_0 \phi_0^*$. Again taking the complex conjugate of Eq.(4.84) and multiplying with

Eq.(4.83), we get

$$\begin{aligned}&\left\{-i\beta E_{Lx}+\left(\omega_L^2-c^2k_L^2-\alpha\right)E_{Ly}\right\}\epsilon_A\\&=-\left(\omega_L E_{Lx}-i\omega_{ce}E_{Ly}\right)\frac{ie}{m_e}\frac{\omega_L\omega_{ce}k_{0x}}{k_{Az}\lambda_{FA}^2F_0\left(\omega_0^2-\omega_{ce}^2\right)}H\left|\phi_0\right|^2\end{aligned}\tag{4.87}$$

Eq.(4.86) and Eq.(4.87) can be rearranged as

$$\begin{aligned}&\left[\left(\omega_L^2-c^2k_{Lz}^2-\alpha\right)\epsilon_A+\frac{e}{m_e}\frac{\omega_L^2\omega_0k_{0x}}{k_{Az}\lambda_{FA}^2F_0\left(\omega_0^2-\omega_{ce}^2\right)}H\left|\phi_0\right|^2\right]E_{Lx}\\&+\left[i\beta\epsilon_A-i\frac{e}{m_e}\frac{\omega_{ce}\omega_L\omega_0k_{0x}}{k_{Az}\lambda_{FA}^2F_0\left(\omega_0^2-\omega_{ce}^2\right)}H\left|\phi_0\right|^2\right]E_{Ly}=0\end{aligned}\tag{4.88}$$

and

$$\begin{aligned}&\left[-i\beta\epsilon_A+\frac{ie}{m_e}\frac{\omega_L^2\omega_{ce}k_{0x}}{k_{Az}\lambda_{FA}^2F_0\left(\omega_0^2-\omega_{ce}^2\right)}H\left|\phi_0\right|^2\right]E_{Lx}\\&+\left[\left(\omega_L^2-c^2k_L^2-\alpha\right)\epsilon_A+\omega_{ce}\frac{e}{m_e}\frac{\omega_L\omega_{ce}k_{0x}}{k_{Az}\lambda_{FA}^2F_0\left(\omega_0^2-\omega_{ce}^2\right)}H\left|\phi_0\right|^2\right]E_{Ly}=0\end{aligned}\tag{4.89}$$

Now, we can easily get the coupled expression of three waves interaction by eliminating E_{Lx} and E_{Ly} from Eqs.(4.88 and 4.89), as

$$D_L\epsilon_A=\mu\tag{4.90}$$

where,

$$\mu=-\frac{\left\{\left(\omega_L^2-c^2k_L^2-\alpha\right)\left(\omega_{ce}^2+\omega_0\omega_L\right)+\beta\omega_{ce}\left(\omega_L+\omega_0\right)\right\}}{\left(\omega_L^2-c^2k_L^2-\alpha-\beta\right)}\frac{e}{m_e}\frac{\omega_Lk_{0x}}{k_{Az}\lambda_{FA}^2F_0\left(\omega_0^2-\omega_{ce}^2\right)}H\left|\phi_0\right|^2\tag{4.91}$$

and

$$D_L=\omega_L^2-c^2k_L^2-\alpha+\beta\tag{4.92}$$

Equation (4.90) describes the coupling of the oblique langmuir wave with the LHCP radiation and the low frequency SAW in spin quantum plasmas. From $D_L=0$, we can get the spin modified linear dispersion relation of LHCP in quantum plasmas.

4.4 Growth Rate

In order to obtain the growth of this three-wave parametric instability in homogeneous spin degenerate magneto-plasmas, we expand $\epsilon_A(\omega_A,\mathbf{k}_A)$ and $D_L(\omega_L,\mathbf{k}_L)$ around the resonant fre-

quencies [12]–[14], [36]–[38],

$$\omega_L = \omega_L + i\gamma, \tag{4.93}$$

$$\omega_A = \omega_A + i\gamma, \tag{4.94}$$

$$\epsilon_A(\omega_A, \mathbf{k}_A) = \epsilon_A^R(\omega_A, \mathbf{k}_A) + i\gamma \frac{\partial \epsilon_A^R}{\partial \omega_A}, \tag{4.95}$$

$$D_L(\omega_L, \mathbf{k}_L) = D_L^R(\omega_L, \mathbf{k}_L) + i\gamma \frac{\partial D_L^R}{\partial \omega_L}, \tag{4.96}$$

where $\gamma << \omega_L, \omega_A$ and the superscript R is for real values. At resonance $\epsilon_A^R = 0$ and $D_L^R = 0$, so Eqs.(4.93–4.96) yield

$$(\gamma + \gamma_{DA})(\gamma + \gamma_{DL}) \equiv -\frac{\mu}{\frac{\partial D_L^R}{\partial \omega_L}\frac{\partial \epsilon_A^R}{\partial \omega_A}} \equiv \gamma^2 \tag{4.97}$$

Here

$$\frac{\partial D_L^R}{\partial \omega_L} = 2\omega_L - \frac{\omega_{ce}\left(\omega_{pe}^2 + c^2 k_{Lz}^2 Sp\right)}{\left(\omega_L + \omega_{ce}\right)^2} \tag{4.98}$$

and

$$\frac{\partial \epsilon_A^R}{\partial \omega_A} = -\frac{2\omega_A}{c^2 k_{Ax} k_{Az}\left(1 - Sp + \frac{v_{ti}^2}{v_A^2}\right)} \left\{ \begin{array}{c} \left(\frac{\omega_A^2}{k_{Az}^2 \lambda_{FA}^2} - \omega_{pi}^2 + c^2 k_{Ax}^2 Sp\right)\left(1 + \frac{c^2}{v_A^2}\right) \\ + \frac{1}{k_{Az}^2 \lambda_{FA}^2}\left(\omega_A^2\left(1 + \frac{c^2}{v_A^2}\right) - c^2 k_{Az}^2 (1 - Sp)\right) \end{array} \right\} \tag{4.99}$$

Now, we make numerical calculations of γ/ω_A as a function of various parameters of interest in a degenerate magneto-plasma.

4.5 Numerical Results and Graphical Description

The numerical appreciation of the results of our theory is achieved from the calculations of the growth rate of three wave instability for the following set of typical parameters of the dense astrophysical environments like white dwarf star, in cgs system of units. For degenerate magneto-plasmas [54, 55]: $T_{Fe} = \hbar^2(3\pi^2 n_{0e})^{2/3}/2k_B m_e > T_e = 1 \times 10^7 K$; $T_i = 10^3 K$; $\phi_0 = 1 statvolt$; $B_0 = (5-6) \times 10^{11} G$ and $n_{0e} = n_{0i} = (0.5-1) \times 10^{29} cm^{-3}$. The angular frequencies and wave vectors of the three waves at fixed angles $\theta_1 = 0.3^0$(is a small angle that EPW has with

respect to z-axis), $\theta_2 = 11.47^0$(is an angle that SAW has with respect to z-axis), $B_0 = 6 \times 10^{11} G$ and $n_{0e} = n_{0i} = 1 \times 10^{29} cm^{-3}$, are $\omega_0 = 1.8497 \times 10^{19} rad/\sec$, $\omega_A = 4.0558 \times 10^{15} rad/\sec$, $\omega_L = 1.8493 \times 10^{19} rad/\sec$, $k_0 = 3.8 \times 10^8 cm^{-1}$, $k_A = 1 \times 10^7 cm^{-1}$ and $k_L = 3.8979 \times 10^8 cm^{-1}$.

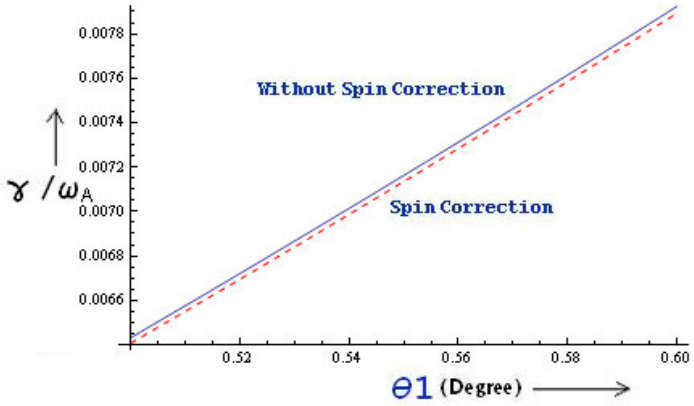

Figure 4-2: Relationship of the normalized growth rate γ/ω_A vs. θ_1.

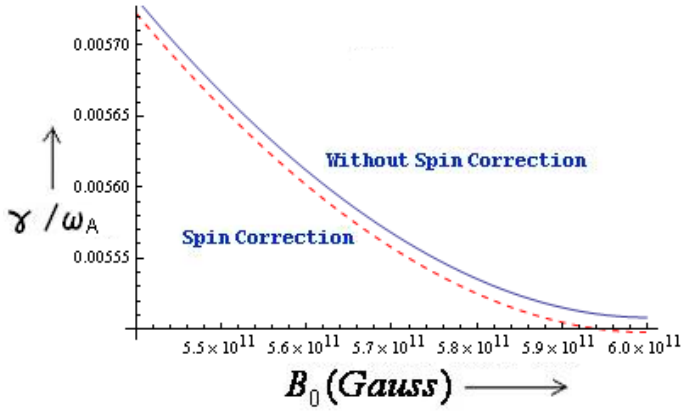

Figure 4-3: Relationship of the normalized growth rate γ/ω_A vs. B_0.

Fig.4-2 elaborates the variation of normalized growth rate γ/ω_A, as a function of angle 'θ_1'. We observe that normalized growth rate increases with the gradual increase in angle.

Fig.4-3 shows the plot of normalized growth rate γ/ω_A for small variations in magnetic field. As we increase the magnetic field from $5.4 \times 10^{11} G$ to $6 \times 10^{11} G$ at $n_{0e} = n_{0i} = 5 \times 10^{28} cm^{-3}$,

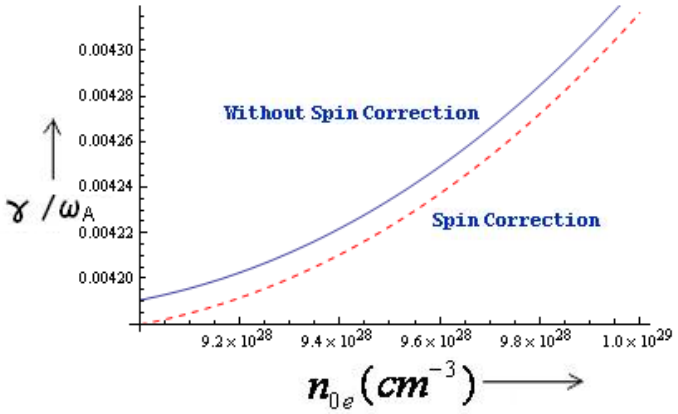

Figure 4-4: Relationship of the normalized growth rate γ/ω_A vs. n_{0e}.

γ/ω_A decreases provided all other parameters remain unchanged. This is because, external magnetic field confines the plasma and tries to reduce the plasma instabilities.

In Fig.4-4 we vary the electron and ion number density and take all other parameters in normalized growth rate as fixed. The normalized growth rate increases with increase in number density from $9 \times 10^{28} cm^{-3}$ to $1 \times 10^{29} cm^{-3}$ at $B_0 = 5.5 \times 10^{11} G$.

We can see that in Figs.(4-2)–(4-4), the normalized growth rate of three wave parametric instability decreases with the inclusion of the spin properties of the electrons. This leads to the stability of the plasma environments. Due to paramagnetic property of spin of electrons, the strength of the external magnetic field increases. As we can see in Fig.4-3 the growth rate decreases with increase of magnetic field, therefore, with spin correction the growth rate decreases in all cases (see Figs.(4-2)–(4-4)).

4.6 Summary

In this chapter we have first time discussed the spin effect on the parametric interaction of oblique Langmuir wave with LHCP and low frequency SAW in non-relativistic homogeneous quantum magneto-plasmas. The QMHD model with quantum effect arising through electron spin dynamics in static magnetic field has been employed to obtain linear and nonlinear response of electrons and ions. Here, electrons with spin-up and spin-down are considered as two different

fluids. The spin contribution does not change the dispersion relation of electrostatic oblique Langmuir wave. This only modifies the dispersion relations of electromagnetic waves (Shear Alfven wave and LHCP). The reason is that *when an electromagnetic perturbation enters the system, the spin-ponderomotive force separates the two populations, which in turn modifies the magnetic field* [55]. The collisions have been neglected in quantum plasmas. This is because, as for high density, $n_{0e} = 1 \times 10^{29} cm^{-3}$, the quantum coupling parameter, $g_Q = \frac{2}{(3\pi^2)^{2/3}} \frac{4\pi e^2 m_e}{\hbar^2 n_{0e}^{1/3}} \approx 0.107845$, but Pauli's blocking comes into play and further reduces the collision rate [18]. At strong magnetic field the Landau quantization or Landau diamagnetization appears but in our case the external magnetic field B_0 is less than quantum critical magnetic field strength $B_Q = 4.4138 \times 10^{13} G$ so $\mu_B B_0 / k_B T_{Fe} < 1$, hence effects of the Landau quantization can be neglected [61].

Chapter 5

Parametric Decay of Oblique Langmuir Wave in High and Low Density Magneto-plasmas

The parametric decay instability of an obliquely propagating Langmuir wave into the low-frequency electromagnetic shear Alfven wave and the Left-Handed Circularly Polarized wave (LHCP) has been investigated in electron-ion plasma, immersed in a uniform external magnetic field. Quantum magneto-hydrodynamic (QMHD) model has been used to find the linear and non-linear response of a high density quantum magneto-plasma. Going to the classical limit ($\hbar \to 0$) retrieves the results for low density classical plasma. Nonlinear dispersion relations and growth rates are analyzed analytically and numerically. It is observed that growth rate in the high density degenerate magneto-plasma increases exponentially while in the low density classical case it increases logarithmically [70].

5.1 Introduction

In this chapter, we discuss the nonlinear interaction of three waves. In this phenomenon an electron plasma wave (EPW) decays parametrically into Left-Handed Circularly Polarized wave and a low-frequency electromagnetic shear Alfven wave (SAW), in a high density (degenerate) magneto-plasma and in a low density (classical) magneto-plasma. The EPW with frequency

ω_0 and wave vector $\mathbf{k}_0$ as a pump is propagating in xz-plane which makes a small angle with z-axis. LHCP propagates along the external magnetic field $B_0\hat{z}$ with frequency ω_L and wave vector $\mathbf{k}_L$, and the excited SAW lies in xz-plane at a small angle with z-axis (See Fig. 5-1).

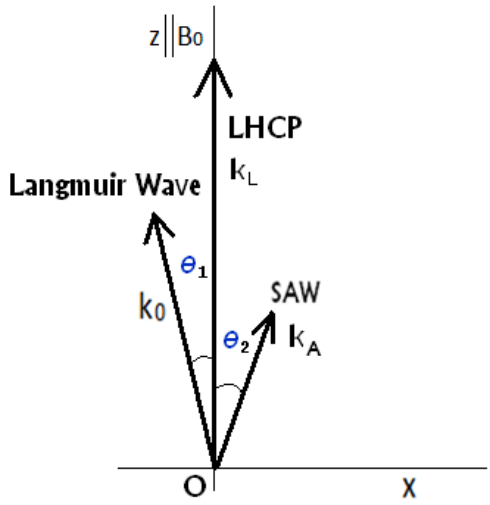

Figure 5-1: Schematic diagram of propagation of EPW, LHCP and SAW in xz-plane.

For quantum magneto-plasmas we use the QMHD model. Quantum effects are only due to electrons where as ions are treated as classical and the following temperature ordering is satisfied, $T_i < T_e < T_{Fe}$. In our problem we consider electrons as a three-dimensional (3D) Fermi gas and the equation of state for such a gas is [28, 73] $P_e = \frac{2}{5}\frac{k_B T_{Fe} n_e^3}{n_{0e}^2}\left[1 + \frac{5}{12}\pi^2\left(\frac{T_e}{T_{Fe}}\right)^2\right]$, where $T_{Fe} = \hbar^2(3\pi^2 n_{0e})^{2/3}/2k_B m_e$ is the electron Fermi temperature and T_e is the electron thermal temperature.

Chapter is organized in the following manner; in Section 5.2 we have introduced the governing equations together with some necessary algebra for each wave mode (EPW, LHCP and SAW). We have derived the linear and nonlinear response functions for the proposed problem. In Section 5.3 nonlinear dispersion relation for three wave interaction has been derived. In Section 5.4 the growth rates of parametric instability for quantum and classical magneto-plasmas have been calculated. The growth rate of parametric instability for the dense astrophysical environments (quantum magneto-plasma) and for the Earth's magnetosphere (classical magneto-plasma) has been plotted in Section 5.5. It is observed that variation of the growth rate against

the number density in the high density degenerate magneto-plasmas increases exponentially while in the low density classical magneto-plasmas it increases logarithmically. Section 5.6 presents the summary of the present work.

5.2 Mathematical Model

Our governing equations for the electrons and ions in the presence of the ambient magnetic field $\mathbf{B}_0 \| \widehat{z}$ are momentum equation, continuity equation and the well known Maxwell's equations.

$$\partial_t \mathbf{v}_j = \frac{q_j \mathbf{E}}{m_j} + \mathbf{v}_j \times \omega_{cj} \widehat{z} - \frac{\nabla P_j}{m_j n_j} + \frac{\hbar^2}{2m_j^2} \nabla \left(\frac{\nabla^2 \sqrt{n_j}}{\sqrt{n_j}} \right), \tag{5.1}$$

$$\partial_t n_j + \nabla . (n_j \mathbf{v}_j) = 0, \tag{5.2}$$

$$\nabla \times \mathbf{E} = -\frac{1}{c} \partial_t \mathbf{B}, \tag{5.3}$$

$$c \nabla \times \mathbf{B} = 4\pi \mathbf{J} + \partial_t \mathbf{E}, \tag{5.4}$$

$$\nabla . \mathbf{E} = 4\pi \sum_j q_j n_j, \tag{5.5}$$

where '$j = e, i$' stands for plasma species. The quantum effects represented in the last term on the right-hand side of Eq.(5.1) are due to the so-called Bohm potential. P_j is the statistical pressure which contains both the Fermi pressure and the thermal pressure [28, 73]. For simplicity, the quantum effects are taken only for electrons whereas ions are treated as classical.

5.2.1 Electron Plasma Wave

We first consider the propagation of a finite amplitude electrostatic EPW in a homogeneous magneto-plasma. The static ambient magnetic field $\mathbf{B}_0$ is along the z-axis. The electric field of the high-frequency wave can be written as

$$\mathbf{E}_0 = (\widehat{x} E_{0x} + \widehat{z} E_{0z}) \exp(-i\omega_0 t + i \mathbf{k}_0 . \mathbf{r}_0) + c.c, \tag{5.6}$$

where $c.c$ stands for the complex conjugate and $E_{0x} < E_{0z}$. The frequency ω_0 and the wave vector $\mathbf{k}_0$ are related by the linear dispersion relation

$$\omega_0^2 = \omega_H^2 + k_0^2 V_{Fe}'^2 - \frac{k_{0z}^2}{k_0^2} \frac{\left(\omega_{pe}^2 + k_0^2 V_{Fe}^2\right) \omega_{ce}^2}{\omega_H^2 + k_0^2 V_{Fe}^2}, \tag{5.7}$$

where $\omega_H^2 = \omega_{pe}^2 + \omega_{ce}^2$, $\omega_{pe}^2 = 4\pi n_{0e} e^2/m_e$, $\omega_{ce} = eB_0/m_e c$, $V_{F0}^2 = V_{Fe}^2 + k_0^2\hbar^2/4m_e^2$, and $V_{Fe}^2 = \frac{6}{5}\frac{k_B T_{Fe}}{m_e}\left[1 + \frac{5}{12}\pi^2\left(\frac{T_e}{T_{Fe}}\right)^2\right]$.

The x- and z-components of the electron velocity and the number density in the field of pump EPW can be determined from equations (5.1 and 5.2) as

$$v_{xe}^0 = -\frac{e\omega_0 k_{0x}\phi_0}{m_e\left(\omega_0^2 - \omega_{ce}^2\right) F_0}, \tag{5.8}$$

$$v_{ze}^0 = -\left(1 + \frac{k_{0x}^2 V_{F0}^2}{(\omega_0^2 - \omega_{ce}^2)F_0}\right)\frac{ek_{0z}\phi_0}{\omega_0 m_e F_0} \tag{5.9}$$

and

$$\frac{n_{1e}^0}{n_{0e}} = -\left(\frac{k_{0z}^2}{\omega_0^2} + \frac{k_{0x}^2}{\left(\omega_0^2 - \omega_{ce}^2\right) F_0}\right)\frac{e\phi_0}{m_e F_0}, \tag{5.10}$$

where $F_0 = 1 - \frac{k_{0z}^2 V_{F0}^2}{\omega_0^2}$, $\frac{k_{0x}^2 V_{F0}^2}{\omega_0^2} << 1$, $E_{0x} = -ik_{0x}\phi_0$ and $E_{0z} = -ik_{0z}\phi_0$.

When the scattered LHCP radiation at $(\omega_L, \mathbf{k}_L)$ propagating exactly parallel to the external magnetic field, beats with the pump wave, it generates a low frequency force which amplifies the Shear Alfven wave at $(\omega_A, \mathbf{k}_A)$. The excited Shear Alfven wave interacts with the pump wave hence generating a nonlinear current which becomes the source of the modified (or amplified) scattered sideband LHCP radiation. These three waves satisfy the following phase matching conditions:

$$\omega_0 = \omega_L + \omega_A, \tag{5.11}$$

$$\mathbf{k}_0 = \mathbf{k}_L - \mathbf{k}_A. \tag{5.12}$$

5.2.2 LHCP Wave

On linearizing the Maxwell equations (5.3 and 5.4) we get the wave equation of the electromagnetic LHCP wave propagating along $\mathbf{B}_0 \| \widehat{z}$,

$$\left(\omega_L^2 - c^2 k_L^2\right) \mathbf{E}_L - i4\pi e \omega_L n_{0e} \mathbf{v}_e^L = -i4\pi \omega_L \mathbf{J}_L^{NL}, \tag{5.13}$$

where

$$\mathbf{J}_L^{NL} = -e \left(n_{1e}^{A*} \mathbf{v}_e^0 + n_{1e}^0 \mathbf{v}_e^{A*}\right) \tag{5.14}$$

is the nonlinear current density due to coupling of EPW and low frequency SAW, which becomes the source to enhance the LHCP radiation. Here, n_{1e}^A and $\mathbf{v}_e^A$ are perturbed electron number density and velocity in the field of SAW. The asterisk denotes the complex conjugate. For LHCP radiation we use $E_{Ly} = -iE_{Lx}$ so that the velocity of electrons in the radiation field can be written as

$$\mathbf{v}_e^L = \frac{-ie}{m_e \left(\omega_L + \omega_{ce}\right)} \mathbf{E}_L. \tag{5.15}$$

By inserting Eq.(5.15) into Eq.(5.13) we get

$$D_L \mathbf{E}_L = -i4\pi \omega_L \mathbf{J}_L^{NL} \tag{5.16}$$

where $D_L = \omega_L^2 - c^2 k_{Lz}^2 - \frac{\omega_{pe}^2 \omega_L}{(\omega_L + \omega_{ce})}$ is the linear dispersion relation of the LHCP. The x-component of the Eq.(5.16) is

$$D_L E_{Lx} = -i4\pi \omega_L J_{Lx}^{NL}, \tag{5.17}$$

here

$$J_{Lx}^{NL} = -e \left(n_{1e}^{A*} v_{xe}^0 + n_{1e}^0 v_{xe}^{A*}\right). \tag{5.18}$$

5.2.3 Shear Alfven Wave

Kinetic Alfven waves [47]–[49], arise in a low-β ($m_e/m_i < \beta = 8\pi n_{0e} k_B T_{eff}/B_0^2 < 1$) plasma with $k_{Az} v_{ti} < \omega_A << \omega_{ci}$, $k_{Az} V_{Fe}$, propagating in xz-plane and making a small angle with $\mathbf{B}_0 \| \widehat{z}$. Here $T_{eff} = \frac{6}{5} T_{Fe} \left[1 + \frac{5}{12}\pi^2 \left(\frac{T_e}{T_{Fe}}\right)^2\right] = m_e V_{Fe}^2/k_B$ and v_{ti} is the ion thermal velocity. The response of the plasma particles due to SAW in this three-wave parametric process, in the

presence of the ambient magnetic field $\mathbf{B}_0$, is governed by the Eq.(5.3) and Eq.(5.4). The wave equation is

$$\left(\omega_A^2 - c^2 k_A^2\right) \mathbf{E}_A + c^2 \left(\mathbf{k}_A . \mathbf{E}_A\right) \mathbf{k}_A - i4\pi e \omega_A n_{0e} \mathbf{v}_e^A + i4\pi e \omega_A n_{0i} \mathbf{v}_i^A = -i4\pi \omega_A \mathbf{J}_A^{NL}, \tag{5.19}$$

where

$$\mathbf{J}_A^{NL} = -e \left(n_{1e}^{L*} \mathbf{v}_e^0 + n_{1e}^0 \mathbf{v}_e^{L*}\right), \tag{5.20}$$

is the nonlinear current density, being generated by the beating of the pump wave and LHCP radiation. Here we take $n_{1e}^L = 0$ due to electromagnetic LHCP radiations. For low frequency electromagnetic SAW, the electrons are inertia less, $k_{Az} >> k_{Ax}$ and also $E_{Ax} >> E_{Az}$. Under these conditions, the perturbed electron number density and the velocity components of species for SAW can be obtained from Eqs.(5.1 and 5.2) as:

$$\frac{n_e^A}{n_{0e}} = \frac{ieE_{Az}}{m_e k_{Az} V_{FA}^2}, \tag{5.21}$$

$$v_{xe}^A \simeq 0, \tag{5.22}$$

$$v_{ze}^A = \frac{ie\omega_A E_{Az}}{m_e k_{Az}^2 V_{FA}^2}, \tag{5.23}$$

$$v_{xi}^A = \frac{-ie\omega_A E_{Ax}}{\omega_{ci}^2 m_i} - \frac{k_{Ax} T_i}{\omega_{ci}^2} \frac{iek_{Az} E_{Az}}{\omega_A m_i^2}, \tag{5.24}$$

and

$$v_{zi}^A = -\frac{iek_{Ax} k_{Az} T_i E_{Ax}}{\omega_{ci}^2 \omega_A m_i^2} + \frac{ieE_{Az}}{\omega_A m_i}. \tag{5.25}$$

Substituting Eqs.(5.22–5.25) into x- and z-components of Eq.(5.19), we get

$$\left(\omega_A^2 - c^2 k_{Az}^2 + \frac{\omega_{pi}^2 \omega_A^2}{\omega_{ci}^2}\right) E_{Ax} + \left(\frac{\omega_{pi}^2}{\omega_{ci}^2} \frac{k_{Ax} k_{Az} T_i}{m_i}\right) E_{Az} = -i4\pi \omega_A J_{Ax}^{NL} \tag{5.26}$$

and

$$\left(c^2 k_{Ax} k_{Az} + \frac{\omega_{pi}^2}{\omega_{ci}^2} \frac{k_{Ax} k_{Az} T_i}{m_i}\right) E_{Ax} + \left(\frac{\omega_A^2}{k_{Az}^2 \lambda_{FA}^2} - \omega_{pi}^2\right) E_{Az} = -i4\pi \omega_A J_{Az}^{NL}, \tag{5.27}$$

where

$$J_{Ax}^{NL} = -en_{1e}^{0} v_{xe}^{L*} \tag{5.28}$$

and

$$J_{Az}^{NL} = 0. \tag{5.29}$$

Here $n_{1e}^{L} = 0$, $v_{ze}^{L} = 0$, $\lambda_{FA}^{2} = \frac{V_{FA}^{2}}{\omega_{pe}^{2}}$, $V_{FA}^{2} = V_{Fe}^{2} + k_{A}^{2}\hbar^{2}/4m_{e}^{2}$ and $k_{Az}^{2}\lambda_{FA}^{2} << 1$. From Eq.(5.27) and Eq.(5.29) we get

$$\left(c^{2}k_{Ax}k_{Az} + \frac{\omega_{pi}^{2}}{\omega_{ci}^{2}}\frac{k_{Ax}k_{Az}T_{i}}{m_{i}}\right)E_{Ax} + \left(\frac{\omega_{A}^{2}}{k_{Az}^{2}\lambda_{FA}^{2}} - \omega_{pi}^{2}\right)E_{Az} = 0. \tag{5.30}$$

Eliminating E_{Ax} from Eqs.(5.26 and 5.30) we left with

$$\epsilon_{A}E_{Az} = -i4\pi\omega_{A}J_{Ax}^{NL}, \tag{5.31}$$

where

$$\epsilon_{A} = \frac{c^{2}}{v_{A}^{2}}k_{Ax}k_{Az}v_{ti}^{2} - \frac{\left(\omega_{A}^{2}\left(1+\frac{c^{2}}{v_{A}^{2}}\right) - c^{2}k_{Az}^{2}\right)\left(\frac{\omega_{A}^{2}}{k_{Az}^{2}\lambda_{FA}^{2}} - \omega_{pi}^{2}\right)}{c^{2}k_{Ax}k_{Az}\left(1+\frac{v_{ti}^{2}}{v_{A}^{2}}\right)}, \tag{5.32}$$

and $v_{A}^{2} = c^{2}\frac{\omega_{ci}^{2}}{\omega_{pi}^{2}}$ is Alfven velocity. By taking $\epsilon_{A} = 0$, we can get the linear dispersion relation of the SAW. The right hand side of the Eq.(5.31) is the coupling of the pump wave and the LHCP which provides the source to enhance the SAW.

5.3 Nonlinear Dispersion Relations

We can now proceed to derive the nonlinear dispersion relation which results from the coupling of the proposed three wave interaction. Using the values of v_{xe}^{0}, n_{1e}^{0}, v_{xe}^{A} and n_{1e}^{A}, from Eqs.(5.8, 5.10, 5.22 and 5.21), into Eq.(5.18) respectively, we get

$$J_{Lx}^{NL} = \frac{-ie}{4\pi m_{e}}\frac{\omega_{0}k_{0x}}{k_{Az}\lambda_{FA}^{2}F_{0}\left(\omega_{0}^{2} - \omega_{ce}^{2}\right)}\phi_{0}E_{Az}^{*} \tag{5.33}$$

Hence, Eq.(5.17) become

$$D_L E_{Lx} = -\frac{e}{m_e} \frac{\omega_L \omega_0 k_{0x}}{k_{Az} \lambda_{FA}^2 F_0 \left(\omega_0^2 - \omega_{ce}^2\right)} \phi_0 E_{Az}^* \tag{5.34}$$

We also need to substitute the value of n_{1e}^0 from Eq.(5.10) and $v_{xe}^L = \frac{-ie}{m_e(\omega_L + \omega_{ce})} E_{Lx}$ into Eq.(5.28) to obtain

$$J_{Ax}^{NL} = \frac{ie}{4\pi m_e} \left(\frac{k_{0z}^2}{\omega_0^2} + \frac{k_{0x}^2}{\left(\omega_0^2 - \omega_{ce}^2\right) F_0} \right) \frac{1}{F_0} \frac{\omega_{pe}^2}{(\omega_r + \omega_{ce})} \phi_0 E_{Lx}^* \tag{5.35}$$

Finally Eq.(5.31) takes the form

$$\epsilon_A E_{Az} = \frac{e}{m_e} \left(\frac{k_{0z}^2}{\omega_0^2} + \frac{k_{0x}^2}{\left(\omega_0^2 - \omega_{ce}^2\right) F_0} \right) \frac{1}{F_0} \frac{\omega_{pe}^2 \omega_A}{(\omega_r + \omega_{ce})} \phi_0 E_{Lx}^*. \tag{5.36}$$

Taking the complex conjugate of Eq.(5.34) and multiplying it with Eq.(5.36), we get the coupled expression for three waves as

$$D_L \epsilon_A = \mu, \tag{5.37}$$

where

$$\mu = -\frac{e^2}{m_e^2} \frac{\omega_L \omega_0 k_{0x} \left|\phi_0\right|^2}{k_{Az} \lambda_{FA}^2 F_0^2 \left(\omega_0^2 - \omega_{ce}^2\right)} \frac{\omega_{pe}^2 \omega_A}{(\omega_L + \omega_{ce})} \left(\frac{k_{0z}^2}{\omega_0^2} + \frac{k_{0x}^2}{\left(\omega_0^2 - \omega_{ce}^2\right) F_0} \right), \tag{5.38}$$

and

$$\left|\phi_0\right|^2 = \phi_0 \phi_0^*. \tag{5.39}$$

Equation (5.37) describes the coupled nonlinear dispersion relation of the oblique langmuir wave, LHCP radiation and the low frequency SAW. The left hand side of the Eq.(5.37) is the product of the linear dispersion relations of LHCP and SAW, and μ is the coupling parameter which mainly comes from the pump wave.

5.4 Growth Rates

In order to obtain the growth rate of this three-wave parametric instability in the homogeneous degenerate magneto-plasmas, we expand $\epsilon_A(\omega_A, \mathbf{k}_A)$ and $D_L(\omega_L, \mathbf{k}_L)$ around the resonant frequencies [12]–[14], [36]–[38],

$$\omega_L = \omega_L + i\gamma, \tag{5.40}$$

$$\omega_A = \omega_A + i\gamma, \tag{5.41}$$

$$\epsilon_A(\omega_A, \mathbf{k}_A) = \epsilon_A^R(\omega_A, \mathbf{k}_A) + i\gamma \frac{\partial \epsilon_A^R}{\partial \omega_A}, \tag{5.42}$$

$$D_L(\omega_L, \mathbf{k}_L) = D_L^R(\omega_L, \mathbf{k}_L) + i\gamma \frac{\partial D_L^R}{\partial \omega_L}, \tag{5.43}$$

where $\gamma << \omega_L, \omega_A$ is the growth rate of the parametric instability and the superscript R is for real values. At resonance $\epsilon_A^R = 0$ and $D_L^R = 0$, so the Eqs.(5.40–5.43) yield

$$(\gamma + \gamma_{DL})(\gamma + \gamma_{DA}) \equiv -\frac{\mu}{\frac{\partial D_L^R}{\partial \omega_L}\frac{\partial \epsilon_A^R}{\partial \omega_A}} \equiv \gamma^2, \tag{5.44}$$

where

$$\frac{\partial D_L^R}{\partial \omega_L} = 2\omega_L - \frac{\omega_{pe}^2 \omega_{ce}}{(\omega_L + \omega_{ce})^2}, \tag{5.45}$$

and

$$\frac{\partial \epsilon_A^R}{\partial \omega_A} = -\frac{2\omega_A \left\{ \frac{1}{k_{Az}^2 \lambda_{Fe}^2} \left(\omega_A^2 \left(1 + \frac{c^2}{v_A^2} \right) - c^2 k_{Az}^2 \right) + \left(\frac{\omega_A^2}{k_{Az}^2 \lambda_{Fe}^2} - \omega_{pi}^2 \right) \left(1 + \frac{c^2}{v_A^2} \right) \right\}}{c^2 k_{Ax} k_{Az} \left(1 + \frac{v_{ti}^2}{v_A^2} \right)}. \tag{5.46}$$

Eq.(5.44) gives the growth rate for degenerate magneto-plasmas. From this equation, we can immediately obtain the growth rate for the classical magneto-plasmas by neglecting the Bohm potential term in Eq.(5.1) and replacing Fermi pressure law $P_e = \frac{2}{5}\frac{k_B T_{Fe} n_e^3}{n_{0e}^2}\left[1 + \frac{5}{12}\pi^2 \left(\frac{T_e}{T_{Fe}}\right)^2\right]$ with $P_{te} = \gamma n_{0e} k_B T_e$, that is replacing λ_{FA}^2 by $\lambda_{De}^2 = \frac{v_{te}^2}{\omega_{pe}^2}$ and F_0 by $F = 1 - \frac{k_{0z}^2 v_{te}^2}{\omega_0^2}$, here $v_{te}^2 = k_B T_e / m_e$. Thus in the classical limit, the expressions (5.38 and 5.46) will be modified as

$$\mu_c = -\frac{e^2}{m_e^2} \frac{\omega_r \omega_0 k_{0x} |\phi_0|^2}{k_{Az} \lambda_{De}^2 F^2 \left(\omega_0^2 - \omega_{ce}^2\right)} \frac{\omega_{pe}^2 \omega_A}{(\omega_r + \omega_{ce})} \left(\frac{k_{0z}^2}{\omega_0^2} + \frac{k_{0x}^2}{\left(\omega_0^2 - \omega_{ce}^2\right) F} \right), \tag{5.47}$$

and

$$\left(\frac{\partial \epsilon_A^R}{\partial \omega_A}\right)_c = -\frac{2\omega_A \left\{ \frac{1}{k_{Az}^2 \lambda_{De}^2} \left(\omega_A^2 \left(1 + \frac{c^2}{v_A^2} \right) - c^2 k_{Az}^2 \right) + \left(\frac{\omega_A^2}{k_{Az}^2 \lambda_{De}^2} - \omega_{pi}^2 \right) \left(1 + \frac{c^2}{v_A^2} \right) \right\}}{c^2 k_{Ax} k_{Az} \left(1 + \frac{v_{ti}^2}{v_A^2} \right)}. \tag{5.48}$$

Finally the growth rate of the three wave interaction for the classical magneto-plasmas becomes

$$\gamma_c^2 \equiv -\frac{\mu_c}{\frac{\partial D_L^R}{\partial \omega_L}\left(\frac{\partial \epsilon_A^R}{\partial \omega_A}\right)_c}. \tag{5.49}$$

Now, we make numerical calculations of γ/ω_A and γ_c/ω_A as a function of various parameters of interest in high and low density magneto-plasmas accordingly.

5.5 Numerical Results and Graphical Description

Now we plot the growth rates of three wave instability for the following set of typical parameters of the dense astrophysical environments like pulsar's magnetosphere, in cgs system of units. For degenerate magneto-plasmas: $T_{Fe} = \hbar^2(3\pi^2 n_{0e})^{2/3}/2k_B m_e >> T_e = 10^3 K$; $T_i = 10^2 K$; $\phi_0 = 1 statvolt$ [54, 55].

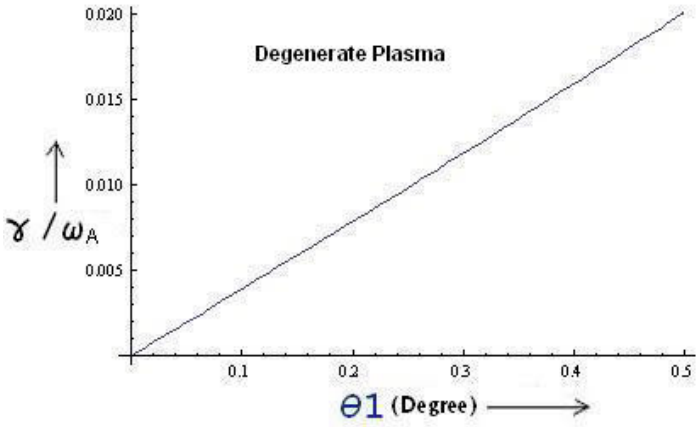

Figure 5-2: Relationship of the normalized growth rate γ/ω_A vs. θ_1 for the high density degenerate magneto-plasmas.

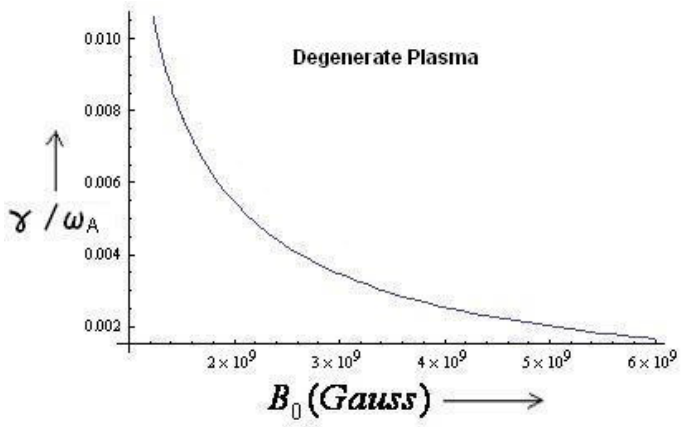

Figure 5-3: Relationship of the normalized growth rate γ/ω_A vs. B_0 for the high density degenerate magneto-plasmas.

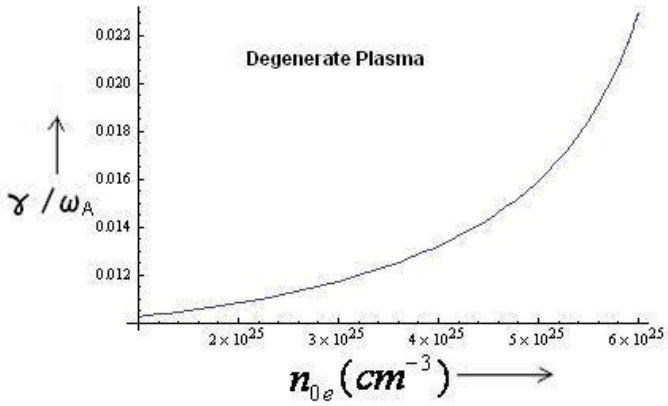

Figure 5-4: Relationship of the normalized growth rate γ/ω_A vs. n_{0e} for the high density degenerate magneto-plasmas.

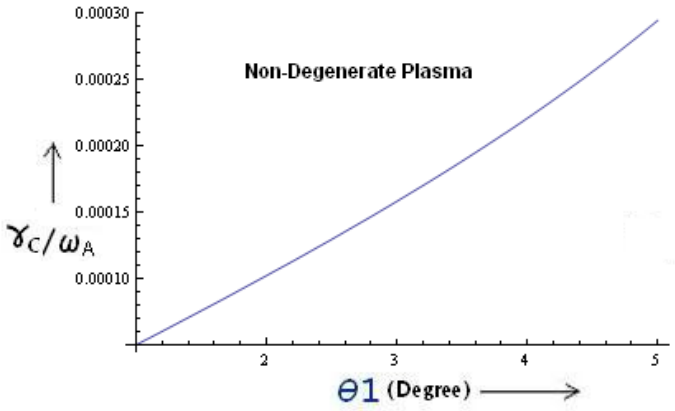

Figure 5-5: Relationship of the normalized growth rate γ_c/ω_A vs. θ_1 for the low density classical magneto-plasmas.

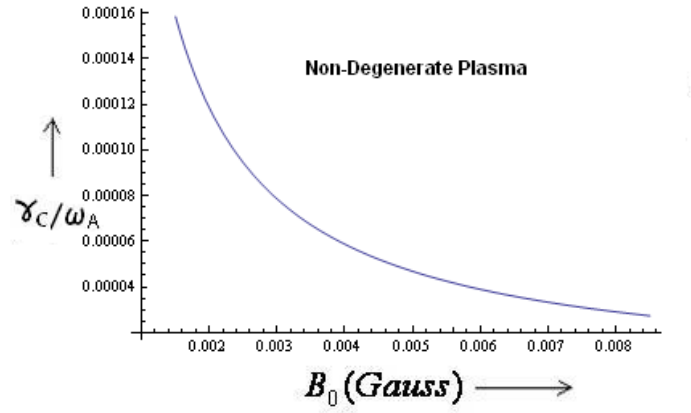

Figure 5-6: Relationship of the normalized growth rate γ_c/ω_A vs. B_0 for the low density classical magneto-plasmas.

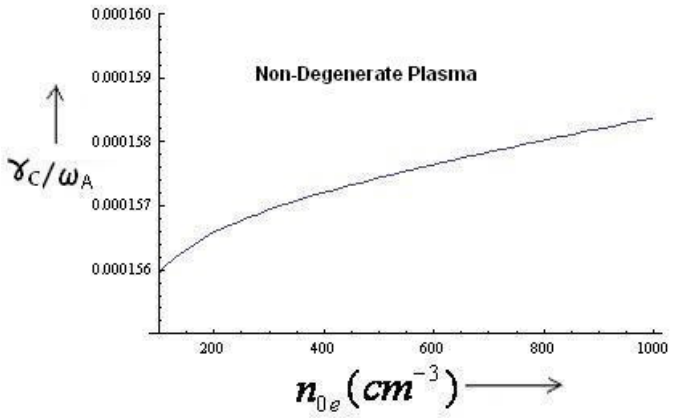

Figure 5-7: Relationship of the normalized growth rate γ_c/ω_A vs. n_{0e} for the low density classical magneto-plasmas.

Fig.5-2 shows the variation of the growth rate γ/ω_A for quantum plasma, as a function of angle 'θ_1' which EPW makes with z-axis. We observe that the growth rate increases with the gradual increase of angle for fixed values of $n_{0e} = n_{0i} = 5 \times 10^{25} cm^{-3}$ and $B_0 = 10^9 G$.

Fig.5-3 exhibits the plot of the growth rate γ/ω_A (quantum plasma) for small variations in magnetic field. As we increase the magnetic field from $1 \times 10^9 G$ to $6 \times 10^9 G$, γ/ω_A decreases provided $n_{0e} = n_{0i} = 5 \times 10^{25} cm^{-3}$, $\theta_1 = 0.4^0$ and $\theta_2 = 10.45^0$ are kept constant. Here, θ_2 is the angle which SAW makes with z-axis.

In Fig.5-4 we vary the electron and ion number density and take all other parameters fixed: $B_0 = 10^9 G$, $\theta_1 = 0.4^0$ and $\theta_2 = 10.45^0$. Plot shows exponential growth in case of quantum plasma regime.

To make a comparison with a low density classical plasma, we select the Earth's magnetospheric environment with plasma parameters in cgs system of units [6, 7]: $T_e = T_i = 1.1604 \times 10^4 K$; $m_i/m_e = 7344$ (for He^+); $E_{0z} = \frac{1}{3} \times 10^{-7} statvolt/cm$; $n_{0e} = n_{0i} = 10^3 cm^{-3}$ and $B_0 = 1.50145 \times 10^{-3} G$.

Fig.5-5 expresses the variation of the growth rate γ_c/ω_A for classical plasma, as a function of angle 'θ_1'. We notice that the growth rate increases with the gradual increase of angle for fixed values of $n_{0e} = n_{0i} = 10^3 cm^{-3}$ and $B_0 = 1.50145 \times 10^{-3} G$.

In Fig.5-6 growth rate γ_c/ω_A decreases with increase of external magnetic field from $B_0 =$

$1.50145 \times 10^{-3}G$ to $B_0 = 8.50145 \times 10^{-3}G$ at $\theta_1 = 3^0$, $\theta_2 = 18.3^0$ and $n_{0e} = n_{0i} = 10^3 cm^{-3}$.

Fig.5-7 represents that the growth rate γ_c/ω_A increases slowly with the increase in number density $n_{0e} = n_{0i} = (0.1-1) \times 10^3 cm^{-3}$ at $\theta_1 = 3^0$ and $\theta_2 = 18.3^0$, in classical magneto-plasma.

We observe that the behavior of the growth rate γ_c/ω_A for classical plasma and that of the growth rate γ/ω_A for quantum plasma is similar as a function of θ_1 (See Fig.5-2 and Fig.5-5) and B_0 (See Fig.5-3 and Fig.5-6), though their magnitudes are different. However, for density variation, the growth rates appear significantly different in classical and quantum magneto-plasma(Compare Fig.5-4 and Fig.5-7). We observe a logarithmic-type of increase in the growth rate for classical plasma as depicted in Fig.5-7. The reason for different behavior of curves in Figs.(5-4)–(5-7) lies in the temperature, which is proportional to the electron number density, $T_{Fe} = \hbar^2(3\pi^2 n_{0e})^{2/3}/2k_B m_e$ for a degenerate plasma but is independent of the density for classical plasma. When number density increases, T_{Fe} also increases, and consequently energy of the system increases rapidly, which in turn results in fast growth. On the other hand, temperature and number density in the classical plasmas are not related to each other. Therefore, with increase in number density the growth rate increases rather slowly and thus the growth in classical plasma varies logarithmically.

5.6 Summary

In this chapter we have discussed the parametric interaction of oblique Langmuir wave with LHCP and the low frequency SAW in both high and low density non-relativistic homogeneous magneto-plasmas. For the high density regime the QMHD model, with quantum effects arising through electron dynamics, has been employed to obtain the linear and nonlinear response of electrons and ions. The collisions have been neglected in quantum plasmas because for high density, $n_{0e} = 5 \times 10^{25} cm^{-3}$, the quantum coupling parameter $g_Q = \frac{2}{(3\pi^2)^{2/3}} \frac{4\pi e^2 m_e}{\hbar^2 n_{0e}^{1/3}} \approx 1.35$, but Pauli's blocking comes into play and further reduces the collision rate [18]. The growth rate, γ/ω_A, for a degenerate magneto-plasma has been plotted for the dense astrophysical environments.

For the low density regime, the classical limit ($\hbar \to 0$, $P_e \to P_{te}$) in the results of QMHD model captures all effects that can be achieved for a classical plasma using fluid model. The

normalized growth rate γ_c/ω_A has been plotted for the Earth's magnetosphere. At fixed value of, $\theta_1 = 3^0$, $\theta_2 = 18.3^0$, $n_{0e} = n_{0i} = 10^3 cm^{-3}$ and $B_0 = 1.50145 \times 10^{-3} G$, the growth rate is $\gamma_c = 1.5 \times 10^{-3}\,\mathrm{sec}^{-1}$. Therefore, it is easy to neglect the Landau damping because in Earth's magnetosphere the collision frequency is rather low ($\nu_{ie} \approx 10^{-4}\,\mathrm{sec}^{-1}$) [6]. The graphical behavior of the growth rate versus angle θ_1 and magnetic field B_0 is the same for both high and low density plasma regimes. On the other hand, the normalized growth rate versus number density ($n_{0e} = n_{0i}$) in the high density degenerate magneto-plasma increases exponentially while in the low density classical magneto-plasma it increases logarithmically. The comparison of Fig.5-4 and Fig.5-7 also shows that the magnitude of the normalized growth rate for the high density quantum regime is some order of magnitude stronger than the normalized growth rate for the low density classical regime.

Chapter 6

Summary and Conclusion

In this chapter, we shall discuss the results of our whole work presented in this thesis. The main theme of this thesis is to study the three wave coupling phenomenon in different plasma environments. The quantum effects due to electrons like degeneracy and spin effect on the growth rate of parametric instability have been highlighted. Two parametric decay processes have been studied. In first process, a finite amplitude electrostatic upper hybrid wave decays parametrically into O-mode and shear Alfven wave in an homogeneous classical magneto-plasma. In second process an oblique Langmuir wave or an electron plasma wave decays parametrically into left hand circular polarized wave and shear Alfven wave in an homogeneous classical, quantum and spin quantum magneto-plasmas.

In chapter 3 we have emphasized that although the spin of electron is a quantum behavior but it can effect the growth rate of parametric interaction of upper hybrid, O-mode and shear Alfven wave even in classical magneto-plasma. Spin effect only modifies the frequencies of electromagnetic waves such as O-mode and shear Alfven wave and it does not change electrostatic upper hybrid wave. The classical fluid model has been extended for spin half particles by taking into account the spin magnetization current and magnetic dipole force. In this three wave interaction UH wave as pump derives O-mode and there is a nonlinear current due to the beating of UH wave with O-mode which becomes the source of energy to amplify the low frequency SAW. The coupling of the excited SAW and UH wave produces another nonlinear current which enhance O-mode radiation. Nonlinear dispersion relation or coupling relation (See Eq.(3.71)) and growth rate (See Eq.(3.74)) of the three wave interaction problem have been derived. The

growth rate is plotted for the typical parameters of fusion plasma. It is clear from Fig.3-4 that growth rate decreases with the inclusion of the spin properties of the electrons. This leads to confine the plasma environment. Spin plays the paramagnetic behavior which is important for the stability of the plasmas. At fixed scattering angles $\theta_1 = 3^0$, $\theta_2 = 0.57^0$ the growth rate $\gamma = 7.3782 \times 10^7\,\mathrm{sec}^{-1}$ is achieved for spin correction and $\gamma = 7.8067 \times 10^7\,\mathrm{sec}^{-1}$ without spin correction. The expression $S_p = \frac{4\pi n_{0e}\mu_B}{B_0} tanh\left(\frac{\mu_B B_0}{k_B T_e}\right)$ and spin magnetization current densities(See Eqs.(3.38, 3.62 and 3.63)) show that the effect of spin on growth rate increases on increasing the n_{0e}. In strongly magnetized homogeneous plasma with high density the spin up population is greater than the spin down population. In this way paramagnetic behavior of spin becomes important even for classical plasma.

In chapter 4 we present the parametric decay of oblique Langmuir wave into low-frequency electromagnetic shear Alfven wave and Left-Handed Circularly Polarized wave in an electron-ion spin quantum plasma immersed in the uniform external magnetic field. The plasma is deeply degenerate such that Fermi temperature is greater than thermal temperature i.e., $T_{Fe} > T_e$, but $T_e \neq 0$, and $T_e > T_i$. The equation of state for 3D electron Fermi gas is taken as [28, 73] $P_e = \frac{2}{5}\frac{k_B T_{Fe} n_e^3}{n_{0e}^2}\left[1 + \frac{5}{12}\pi^2\left(\frac{T_e}{T_{Fe}}\right)^2\right]$. The quantum effects due to electrons like spin, Fermi pressure, Bohm potential have been taken into account and ions are supposed classical. The quantum hydrodynamic model has been used to study the linear and nonlinear response of the plasma species for three-wave coupling interaction in quantum magneto-plasmas. Spin up and spin down electrons are taken as two different fluids and the population difference in degenerate plasma is $n_{0+} - n_{0-} = n_{0e}\frac{3}{2}\frac{\mu_B B_0}{k_B T_{Fe}}$. In this wave interaction phenomenon oblique Langmuir wave which is propagating obliquely to $\mathbf{B}_0 \| \widehat{z}$, derives high frequency LHCP and generating a nonlinear current $\mathbf{J}_A^{NL}$ due to beating of these two waves. This nonlinear current provides an energy source to amplify a low frequency SAW. Latter interacts with Langmuir wave and generating a nonlinear current $\mathbf{J}_L^{NL}$ which becomes the source of LHCP. In this three wave interaction Langmuir wave decays and both LHCP and SAW grow. Here LHCP is propagating parallel to $\mathbf{B}_0 \| \widehat{z}$ and SAW makes a small angle with magnetic field as shown in Fig.4-1. We have derived spin modified nonlinear dispersion relations and growth rate of instability process. The growth rate of three wave instability has been plotted for typical parameters of the dense astrophysical environments like white dwarf star [54, 55]. The normalized growth

rate of three wave parametric instability increases with plasma number density and decreases with ambient magnetic field(see Figs.4-3–4-4). Magnitude of normalized growth rate decreases with the inclusion of the spin properties of the electrons as depicted in Figs.4-2–4-4. This leads to the stability of the plasma environments, since plasma is strongly magnetized. In strong magnetic field spin up population becomes dominant and hence paramagnetic property of spin of electrons gives strength to the external magnetic field which in turn decreases the growth rate. Plasma regime is strongly magnetized but magnetic field is less than quantum critical magnetic field $B_Q = 4.4138 \times 10^{13} G$ and plasma is dense but it is collisionless as quantum coupling parameter is not so large i.e., $g_Q \approx 0.107845$.

Finally, in chapter 5 the parametric decay instability of oblique Langmuir wave into low-frequency electromagnetic shear Alfven wave and Left-Handed Circularly Polarized wave have also been investigated in detail in high density (quantum) and low density (classical) magneto-plasma environments. The wave interaction process is same as discussed in chapter 4 but in this case we have not included the spin of electrons. Electrons are degenerate and dispersive properties of electrons have been dealt by including Bohm potential while ions are thermal. Nonlinear dispersion relation (See Eq.(5.37)) and growth rate (See Eq.(5.44)) of the three wave interaction problem have been derived analytically by using quantum fluid model. To compare the results with the low density classical plasma we have used classical limit ($\hbar \to 0$, $P_e \to P_{te}$) in the results of quantum fluid model (See Eq.(5.49)). For high density plasma regime we have selected the dense astrophysical environments like pulsar's magneto-sphere and for low density plasma regime the Earth's magneto-sphere has been selected. The growth rate both for quantum and classical magneto-plasma environments has been plotted. Growth rate increases with increase in angle of pump wave with $\mathbf{B}_0$ and it decreases with increase of external magnetic field in both quantum and classical magneto-plasmas. Thus the variation of growth rate as a function of θ_1 and B_0 is similar in both quantum and classical plasmas (though its magnitude becomes different). The normalized growth rate in the high density degenerate magneto-plasmas increases exponentially with increase of number density while in the low density classical magneto-plasmas it increases logarithmically with increase of number density as shown in Fig.5-4 and Fig.5-7. The reason behind is that Fermi temperature depends on number density in degenerate plasma while in classical plasma temperature and number

density are independent to each other. Therefore in quantum plasma on increasing the number density T_{Fe} increases, in turn system gets energy rapidly and growth rate increases fastly while in classical plasma on increasing number density, the temperature remain constant and growth rate increases rather slowly.

For degenerate electrons (in chapters 4 & 5), the limitation $k\lambda_F << 1$ on the wavelengths has been used which describes the applicability range of quantum hydrodynamics equations. The quantum hydrodynamic model correctly describes the dispersion of longitudinal oscillations in degenerate electron gas for the wavelengths of wave phenomena be larger than Thomas-Fermi length, $k\lambda_F << 1$ [87].

In all three wave interaction processes, in this thesis, excited low frequency wave is shear Alfven wave. As Alfven waves are commonly used for plasma heating. Particularly, in chapter 5 we have discussed the decay of EPW into LHCP and SAW in Earth's magneto-sphere. The excited SAW may travel towards pole and heat the plasma which results in the generation of Auroral kilometric radiations (O-mode or LHCP).

Bibliography

[1] F. F. Chen, *Introduction to Plasma Physics and Controlled Fusion*, vol. **1** (Plenum Press, New York, 1984).

[2] P. K. Shukla and A. A. Mamun, *Introduction to Dusty plasma Physics*, Institute of Physics Bristol and Philadelphia, (2001).

[3] W. L. Kruer, *The Physics of Laser Plasma Interactions*, (Addison-Wesley Publishing Company, p.2–138, 1988).

[4] J. F. Drake, P. K. Kaw, Y. C. Lee, G. Schmid, C. S. Liu, and M. N. Rosenbluth, Phys. Fluids **17**, 778 (1974).

[5] R. P. Sharma and P. K. Shukla, Phys. Fluids **26**, 87 (1983).

[6] G. Murtaza and P. K. Shukla, J. Plasma Physics **31**, 423 (1984).

[7] H. Saleem, M. B. Chaudhry, G. Murtaza, and P. K. Shukla, Phys. Fluids **28**, 3 (1985).

[8] S. V. Vladimirov and S. I. Popel, Phys. Scripta **50**, 161 (1994).

[9] K. Tanaka, L. M. Goldman, W. Seka, M. C. Richardson, J. M. Soures, and E. A. Williams, Phys. Rev. Lett., **48**, 1179 (1982).

[10] M. Salimullah and M. H. A. Hassan, Phys. Rev. A., **41**, 6963 (1990).

[11] M. P. Hetrzberg, N. F. Cramer, and S. V. Vladimirov, Phys. Plasmas **10**, 3160 (2003).

[12] M. Jamil, H. A. Shah, M. Salimullah, K. Zubia, I. Zeba, and Ch. Uzma, Phys. Plasmas **17**, 073703 (2010).

[13] M. K. Islam, M. Salahuddin, T. Ferdous, and M. Salimullah, Phys. Scr. **61**, 485 (2000).

[14] M. Jamil, M. Shahid, Waris Ali, M. Salimullah, H. A. Shah, and G. Murtaza, Phys. Plasmas **18**, 063705 (2011).

[15] P. K. Shukla and B. Eliasson, Phys. Rev. Lett. **99**, 096401 (2007).

[16] P. K. Shukla, S. Ali, L. Stenflo and M. Marklund, Phys. Plasmas **13**, 112111 (2006).

[17] F. Haas, Europhys. Lett. **77**, 45004 (2007).

[18] G. Manfredi, Fields Inst. Commun. **46**, 263 (2005).

[19] L. G. Garcia, F. Haas, L. P. L de Oliveira, and J. Goedert, Phys. Plasmas **12**, 012302 (2005).

[20] P. K. Shukla and B. Eliasson, Phys. Rev. Lett. **96**, 245001 (2006).

[21] D. Shaikh and P. K. Shukla, Phys. Rev. Lett. **99**, 125002 (2007).

[22] F. Haas, Phys. Plasmas **12**, 062117 (2005).

[23] F. Haas, L. G. Garcia, J. Goedert, and G. Manfredi, Phys. Plasmas **10**, 3858 (2003).

[24] P. K. Shukla and L. Stenflo, Phys. Lett. A **357**, 229 (2006).

[25] W. Li and Y. N. Wang, Phys. Rev. B **75**, 193407 (2007).

[26] F. Haas, G. Manfredi, and M. R. Feix, Phys. Rev. E **62**, 2763 (2000).

[27] M. Jamil, M. Shahid, I. Zeba, M. Salimullah, H. A. Shah, and G. Murtaza, Phys. Plasmas **19**, 023705 (2012).

[28] Zhengwei Wu, Haijun Ren, Jintao Cao, and P. K. Chu, Phys. Plasmas **15**, 082103 (2008).

[29] F. Haas, Phys. Plasmas **15**, 022104 (2008).

[30] A. Bret and F. Haas Phys. Plasmas **17**, 052101 (2010).

[31] M. F. Bashir, M. Jamil, G. Murtaza, M. Salimullah, and H. A. Shah, Phys. Plasmas **19**, 043701 (2012).

[32] R. S. Fletcher, X. L. Zhang, and S. L. Rolston, Phys. Rev. Lett. **96**, 105003 (2006).

[33] W. Li, P. J. Tanner, and T. F. Gallagher, Phys. Rev. Lett. **94**, 173001 (2005).

[34] N. Crouseilles, P. A. Hervieux, and G. Manfredi, Phys. Rev. B **78**, 155412 (2008).

[35] Y. D. Jung, Phys. Plasma **8**, 3842 (2001).

[36] H. G. Craighead, Science **290**, 1532 (2000).

[37] P. A. Norreys, F. N. Beg, Y. Sentoku, L. O. Silva, R. A. Smith, and R. M. G. M. Trines, Phys. Plasmas **16**, 041002 (2009).

[38] A. Y. Wong and R. J. Taylor, Phys. Rev. Lett. **27**, 644 (1971).

[39] V. V. Migulin and A. V. Gurevich, J. Atoms. Terr. Phys. **47**, 1181 (1984).

[40] W. Scales and P. Kinter, J. Geophys. Res. **95**, 10623 (1990).

[41] J. A. Fejer, M. P. Sulzer, and J. H. Eddler, J. Geophys. Res. **96**, 15985 (1991).

[42] P. Stubbe, H. Kohl, and M. T. Rietveld, J. Geophys. Res. **97**, 6285 (1992).

[43] A. J. Stocker, et al., J. Atoms. Terr. Phys. **54**, 1555 (1992).

[44] M. Y. Yu and P. K. Shukla, Plasmas Phys. **19**, 889 (1977).

[45] K. B. Dysthe, E. Mjolhus, H. L. Pecseli, and L. Stenflo, Plasmas Phys. **20**, 1087 (1978).

[46] P. A. Markowich, C. A. Ringhofer, and C. Schmeiser, *Semiconductor Equations* (Springer-Verlag, New York, 1990).

[47] M. F. Bashir, Z. Iqbal, I. Aslam, and G. Murtaza, Phys. Plasmas **17**, 102112 (2010).

[48] R. L. Lysak and W. Lotko, J. Geophys. Res., **101**, 5085 (1996).

[49] Neil F. Cramer, *The Physics of Alfven Waves*, (Wiley, Berlin, 2001).

[50] M. Iannuzzi, Phys. Lett. A **30,** 423 (1969).

[51] G. Brodin and M. Marklund, New J. Phys. **9**, 277 (2007).

[52] G. Brodin and M. Marklund, Phys. Plasmas **14**, 112107 (2007).

[53] G. Brodin and M. Marklund, New J. Phys. **10**, 115031 (2008).

[54] A. P. Misra, G. Brodin, M. Marklund, and P. K. Shukla, J. Plasma Physics **76**, 857 (2010).

[55] G. Brodin, M. Marklund, and G. Manfredi, Phys. Rev. Lett. **100**, 175001 (2008).

[56] Felipe A. Asenjo, Jens Zamanian, M. Marklund, G. Brodin, and Petter Johansson, New J. Phys. **14**, 073042 (2012).

[57] G. Brodin, J. Lundin, J. Zamanian, and M. Stefan, New J. Phys. **13**, 083017 (2011).

[58] M. Marklund and G. Brodin, Phys. Rev. Lett. **98**, 025001 (2007).

[59] Felipe A. Asenjo, Victor Munoz, J. Alejandro Valdivia, and Swadesh M. Mahajan, Phys. Plasmas **18**, 012107 (2011).

[60] A. Hussain, Z. Iqbal, G. Brodin, and G. Murtaza, Phys. Lett. A **377,** 2131 (2013).

[61] J. Zamanian, M. Marklund, and G. Brodin, New J. Phys. **12,** 043019 (2010).

[62] Mubashar Iqbal, J. Plasma Physics **79**, p. 19-23 (2013).

[63] P. A. Polyakov, Russ. Phys. J. **22**, 310 (1979).

[64] L. W. Brown, Astrophys. J. **180**, 359, (1973).

[65] M. Shahid, D. B. Melrose, M. Jamil, and G. Murtaza, Phys. Plasmas **19**, 112114 (2012).

[66] L. D. Landau and E. M. Lifshitz, *Statistical Physics*. Part I (Pergamon, Oxford, 1978).

[67] V. S. Rastunkov and V. P. Krainov, Phys. Rev. E **69**, 037402 (2004).

[68] M. Shahid and G. Murtaza, Phys. Plasmas **20**, 082124 (2013).

[69] A. N. Kaufman and L. Stenflo, Phys. Scr. **11**, 269 (1975).

[70] M. Shahid, A. Hussain, and G. Murtaza, Phys. Plasmas **20**, 092121 (2013).

[71] S. O. Pillai, *Solid State Physics*, Ed., **6**, (New Age International Publishers, New Delhi, 2006).

[72] A. Dinklage, T. Klinger, G. Marx, and L. Schweikhard, *Plasma Physics, Lect. Notes* Phys. **670**, (Springer, Berlin Heidelberg, 2005).

[73] M. Kardar, Statistical Physics of Particles (Cambridge University Press, New York, 2007).

[74] D. A. Gurnett and R. R. Shaw, J. Geophys. Res. **78**, 8136 (1973).

[75] D. D. Barbosa, Rev. Geophys. Space Phys. **20**, 316 (1982).

[76] D. B. Melrose, J. Geophys. Res. **86**, 30 (1981).

[77] J. Etcheto, P. J. Christiansen, M. P. Gough, and J. G. Trotignon, Geophys. Res. Lett. **9**, 1239 (1982).

[78] M. P. Gough, Planet. Space Sci. **30**, 657 (1982).

[79] W. S. Kurth, J. D. Craven, L. A. Frank, and D. A. Gurnett, J. Geophys. Res. **84**, 4145 (1979).

[80] W. S. Kurth, Geophys. Res. Lett. **9**, 1341 (1982).

[81] M. P. Gough, P. J. Christiansen, and R. Thomas, Adv. Space Sci. **1**, 345 (1981).

[82] W. S. Kurth, D. A. Gurnett, and R. R. Anderson, J. Geophys. Res. **86**, 5519 (1981).

[83] S. D. Shawhan, Rev. Geophys. Space Phys. **17**, 705 (1979).

[84] P. J. Christiansen, J. Etcheto, K. Ronnmabk, and L. Stenflo, Geophys. Res. Lett. **11**, 139 (1984).

[85] J. Weiland and H. Wilhelmsson, *Coherent Nonlinear Interactions of Waves in Plasmas*, (Pergamon, Oxford, 1977).

[86] B. B. Kadomtsev, *Cooperative effects in plasmas, in Reviews of Plasma Physics*, vol. 22, ed. by V. D. Shafranov (Kluwer Academic/Consultants Bureau, New York, 2001).

[87] S. V. Vladimirov and Yu O Tyshetskiy, Physics-Uspekhi **54** (12) 1243-1256 (2011).